Karlsruhe Institute of Technology

cuaa-dahz
deutsch-argentinisches hochschulzentrum
centro universitario argentino-alemán

ITBA
Instituto Tecnológico de Buenos Aires

Master Thesis

Experimental set-up for bubble behaviour in a high pressure alkaline electrolyte

Felix Frey

Matriculation Number: 1911019

Examiner: Prof. Dr.-Ing. Thomas Schulenberg
Dra.-Ing. Cecilia Smoglie

Tutor: Dr. Ing. Thomas Jordan
Dr. Ing. Perdo Orbaiz

Karlsruhe, 31. May 2016

Declaration of Authorship

I declare that I have developed and written the enclosed Master Thesis completely by myself, and have not used sources or means without declaration in the text. Any thoughts from others or literal quotations are clearly marked. The Master Thesis was not used in the same or in a similar version to achieve an academic grading or is being published elsewhere.

Karlsruhe, 31.5.2016

Place, Date | Signature

Abstract

English

The increase in the proportion of renewable energy in the energy matrix and associated unpredictable electricity surpluses, the need for efficient forms of energy storage raises. Due to high energy density and transportability, hydrogen plays an important role as energy storage.
After the production of hydrogen by electrolysis a significant percentage of the stored energy is used for the compression of the hydrogen gas. Higher efficiencies are reached by high pressure electrolysis, because subsequently compression of the hydrogen gas is not necessary.
In the course of a cooperation between the Institute of Nuclear and Energy Technologies (IKET) and the Instituto Tecnológico de Buenos Aires (ITBA), a high pressure electrolyser Experiment has been developed at ITBA. The particularity about this device besides the high working pressure, are glass windows in the taps in order to be able to analyse the behaviour of the gas bubbles. Experiments for the investigation of the bubble behaviour have been performed at IKET.
This master thesis describes the development of the project, from the design and construction of the electrolyser at ITBA, to the execution of first series of experiments at IKET. First conclusions about the bubble behaviour are presented.

Deutsch

Durch den Anstieg des Anteils der erneuerbaren Energien am Energiemix und die einhergehenden Stromüberschüsse steigt die Notwendigkeit an zur Speicherung elektrischer Energie. Wasserstoff kommt dabei als chemischer Energiespeicher aufgrund seiner hohen Energiedichte und vielfältiger Nutzbarkeit eine wichtige Rolle zu.

Nach der Herstellung des Wasserstoffs, z.B. mittels Elektrolyse ("Power-to-Gas"), wird ein bedeutender energetischer Aufwand für die Verdichtung bis zu den notwendigen Speicherdrücken von mehreren hundert bar aufgebracht. Höhere Effizienz weißt die Elektrolyse unter hohen Drücken auf, da hier die Gase bereits bei relativ hohen Drücken erzeugt werden.
Im Zuge einer Kooperation des Instituts für Kern und Energietechnik (IKET) und dem Instituto Tecnológico de Buenos Aires (ITBA), wurde ein Experiment zur alkalischen Hochdruckelektrolyse entwickelt. Die Besonderheit dieses Experiments sind Glasfester, die einen direkten optischen Zugang bei hohen Arbeitsdrücken erlauben. Im Rahmen dieser Arbeit wurden erste Experimente zur Untersuchung der Eigenschaften bzw. des Verhaltens von Wasserstoff und Sauerstoff im flüssigen alkalischen Elektrolyt durchgeführt.
Diese Masterarbeit beschreibt die Entwicklung der Elektrolysezelle am ITBA, die Einrichtung der Messtechnik und die Durchführung erster Versuchsreihen am IKET. Erste Ergebnisse bezüglich Blasenverhalten und Blaseneigenschaften werden dargestellt.

Español

El aumento de la proporción de energías renovables en la matriz energética y los excedentes de electricidad impredecibles asociados causan la necesidad de formas eficientes de almacenamiento de energía.
Debido a la alta densidad de energía y facilidad de transporte, el hidrógeno tiene un rol importante como almacenamiento de energía. Después de la producción de hidrógeno por electrólisis y compresión posterior para el almacenamiento, un porcentaje significante de la energía almacenada se usa para la compresión del hidrógeno gaseoso. Eficiencias más altas se alcanzan a través de la electrólisis a alta presión, dado que la compresión posterior del hidrogeno no es necesario.
En el curso de una colaboración entre el Institute of Nuclear and Energy Technologies (IKET) y el Instituto Tecnológico de Buenos Aires (ITBA), un electrolizador de alta presiones fue desarrollado en el ITBA. La particularidad de este dispositivo, además de la alta presión, son ventanas de vidrio en las tapas con el fin de poder analizar el comportamiento de las burbujas. Experimentos para investigar el comportamiento de las burbujas han sido realizados en el IKET.
Esta tesis de maestría describe el desarrollo del proyecto, desde el diseño y la construc-

ción del electrolizador en el ITBA, hasta la ejecución de primeras series de experimentos en el IKET. Primeras conclusiones sobre el comportamiento de las burbujas de hidrógeno deben ser hechos.

Contents

List of Figures

1 Introduction

Limited reserves of fossil energy sources, climate change and the nuclear accident in Fukushima in 2011 led in Germany to a politically forced nuclear phase out, accompanied by a shift from fossil energy to renewable energies.
This has recently lead to a massive propagation of renewable energy projects, mainly wind and photovoltaic power generation. One key problem in this transformation is the difficulty to adjust the generation of electrical energy to the demand. In order to stabilize the grid, and to balance the daily and seasonal schemes electricity has to be stored. There are different ways to store energy like mechanical storage as for example pumped storage hydro power stations, or chemical storage which save energy in form of a chemical bond and can be released by a chemical reaction as used in batteries.
One way of chemical energy storage are electrolysers that can use electricity in order to produce hydrogen, which can be stored in tanks ("power-to-gas"). By the oxydising the hydrogen the energy can be recovered. The only products resulting by the exothermic reaction of hydrogen and oxygen is water and energy. This makes hydrogen important for future clean mobility. Cars, trucks and buses powered by hydrogen fuel cells will decrease CO_2 and fine dust waste especially in cities.
Hydrogen is not an energy source, because it is not a gas directly available in nature. In fact it is to be considered a energy storage with excellent properties regarding transportability and energy density per mass unit. Furthermore, if hydrogen is produced from renewable energies it has a minimal CO_2 footprint [1]. This is why hydrogen can play an important role as energy storage, which is necessary on the way to realize the exit from nuclear and fossil-fuel energy.

To lower the costs for transportation and storage hydrogen gas has to be stored under high pressure. Hydrogen produced by electrolysers under ambient conditions has to be compressed to a suitable storage pressure in a thermodynamically complex and energy

consuming procedure. High pressure electrolysers have the advantage that the produced gas already has a high pressure, so there is no need for an additional pressurisation. Though this system has advantages regarding the efficiency. Several problems are induced with increasing pressure. Diffusive losses increase and the transport of the two phase mixtures, considering of hydrogen and oxygen bubbles in the liquid electrolyte becomes less effective. The size of the produced oxygen and hydrogen gas bubbles reduce their diameter as the pressure rises. This leads to a reduced buoyant velocity and to difficulties separating the gas and the liquid at the phase separator.
At the Institute for Nuclear and Energy Technologies (IKET) in Karlsruhe, cand. Ph.D. Michael Ranft has implemented a numerical two-phase model in OpenFOAM in order to simulate the behaviour of the bubbles in the electrolyte. The main target is to predict how the gas raises after leaving the electrode and destruction of the gas bubbles at the free surface.
In order to validate the numerical model, the IKET worked together with the Instituto Tecnológico de Buenos Aires (ITBA) on the experimental set-up of an optically accessible high-pressure electrolyser cell. Main requirements to this electrolyser is a working pressure up to $45MPa$, and windows which allow the observation of the experiment procedure. The product design including construction and first functional tests have been made at the department of energy at ITBA in Argentina. Further experiments with the optical electrolyser have been realized at IKET in Karlsruhe.
In this master thesis I describe my contribution to the design, construction and set-up of the electrolyser, such as the first stage of experiments realized at the KIT. Main objective of the experiments executed in this work is the analysis of the bubble behaviour, statistics of in rising velocity and diameter at increasing working pressures.

2 Theorical Backround

In the following chapter the theoretical backgrounds about water electrolysis in general and high-pressure electrolysis in particular such as the gas bubble behaviour in a liquid electrolyte under changing pressures will be described.

2.1 Electrolysis

Electrolysis describes the process, in which electrical current forces the splitting of a chemical compound into its components. Water electrolysis is the splitting of water into its compounds hydrogen and oxygen. Electrolyses always requires direct current to provide the electrical energy for the chemical endothermic reaction. The reverse process occurs in a fuel cell, converting the chemical energy stored in the hydrogen, into electrical current by the reaction with oxygen.
Basic features of an electrolyser are rather simple. Two electrodes, the positively charged anode and the negatively charged cathode are submerged in the electrolyte. The electrodes are separated via a semi-permeable membrane which allows a flow of ions but prevents the mixing of the gases. In order to provide a sufficient amount of ions for the conduction, which normal water is not able to, acid or alkaline solutions are used as electrolyte.
The typical energy required by bipolar-alkaline-electrolysers is between $4-4.5 kWh/Nm^3 H_2$, operating with an efficiency of about 80%. The production normally occurs at conditions between $70-90°C$, a cell voltage of $1.85-2.05V$ and a current density of 2 to $3 kA/m^2$. A production rate of ca.$500 Nm^3 H_2$ requires $2MW$ of electrical power. The achieved purenesses are 99.9% and 99.8% for hydrogen and oxygen respectively. Production rates are between 20 and $5000 Nm^3/h$. Bigger units are compiled in a modular way. One of the major installations is operating in Egypt producing $33000 Nm^3/h$ [14].

General equations for water electrolysis

The basic equation of splitting water into hydrogen and oxygen through the reaction is shown in eqs. (2.1) to (2.3)
Due to the influence of the electricity hydrogen and oxygen are produced from liquid water as shown in eq. (2.1). Equations (2.2) and (2.3) show the partial reactions taking place at the cathode and the anode respectively. Two electrons are required to produce one hydrogen molecule. See eq. (2.2).

The total reaction is the following:

$$\mathrm{H_2O} \longrightarrow \mathrm{H_2} + \tfrac{1}{2}\,\mathrm{O_2} \tag{2.1}$$

The reaction taking place at the cathode:

$$2\,\mathrm{H_20\,(l)} + 2\,\mathrm{e^-} \longrightarrow \mathrm{H_2(g)} + 2\,\mathrm{OH^-(aq)} \tag{2.2}$$

And the reaction taking place at the anode:

$$2\,\mathrm{OH^-(aq)} \longrightarrow \tfrac{1}{2}\mathrm{O_2(g)} + \mathrm{H_2O(l)} + 2\,\mathrm{e^-} \tag{2.3}$$

The enthalpy of formation ΔH may be split into a reversible and irreversible part as shown in eq. (2.4).

$$\Delta H(t,p) = \Delta G(t,p) + T\Delta S(t,p) \tag{2.4}$$

The theoretical required reversible voltage V_{rev} at normal conditions ($T_0 = 298.15K$ and $p_0 = 101.3kPa$) is calculated with the free enthalpy ΔG, the Faraday constant $F = 96487As/mol$ and n number of electrons (in this case $n = 2$), Eq (2.5).
Taking into account that the heat required to realize the reaction has to be supplied as well by the electric current, the equation (2.5) has to be extended by the term $T\Delta S(t,p)$ in order to calculate the theoretical non-reversible voltage at normal conditions, Eq. (2.6).

$$V_{rev} = \frac{\Delta G}{nF} = 1.23V \tag{2.5}$$

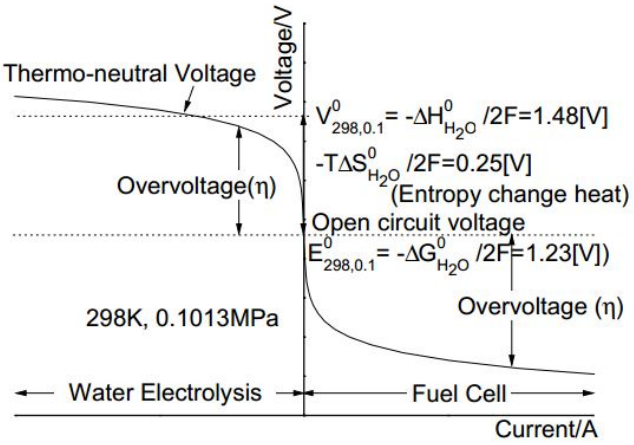

Figure 2.1: Voltage-Current characteristics for water electrolysis and fuel cell.[3]

$$V_{th} = \frac{\Delta G + T\Delta S}{nF} = 1.48V \tag{2.6}$$

In figure (2.1) the voltage and current$(V - I)$ characteristics for fuel cell operation and water electrolysis is graphically illustrated. The right side of the graphic represents a fuel cell and the region on the left side represents water electrolysis.

High pressure electrolysis

As briefly mentioned before, there are three principal ways to store and transport hydrogen; in solid, liquid or gaseous form.
When stored in solid stage, hydrogen gas is getting absorbed in mostly metallic hydrides. This materials are heavy and still expensive. Storage in a liquid form demands a high input of energy for cooling down the gas to the required temperature for liquefaction (20.39 K at 101.3 kPa).
In order to achieve an economically reasonable energy vector in case of gaseous storage the gas has to be compressed. In a study published by Ricardo Lauretta, it is shown that best storage efficiencies are reached at a pressure of about $70MPa$ in case of H_2 [2]. Storage efficiency is defined in Eq. (2.7), with ξ being the storage efficiency, V_n the normal volume of the contained gas $[m^3]$, m the container mass$[kg]$ and ν the container volume $[m^3]$.

$$\xi = \frac{V_n^2}{m\nu} \tag{2.7}$$

Compressors utilized to pressurize the gas demand a high amount of energy. 12 % of the energy stored in hydrogen is required for the pressurization from atmospheric pressure to $30bar$, 29% for the compression up to $200bar$ and 49% for $700bar$, respectively.
High pressure electrolysis produces hydrogen and oxygen gas at high pressures which can be directly stored without the need of further compression. As the electrolyte is an incompressible liquid it demands far less energy to be compressed and the total efficiency of the electrolysis including pressurisation can be seriously reduced. According to studies published by Kazuo Oanda realizing high pressure electrolysis at $70MPa$ requires 5% less energy than a electrolysis at ambient pressure with subsequent compressing of the gas in a second step to $70MPa$. Assuming an efficiency of pump and compressor of 50% [3]. Furthermore compressors are complex and costly technologies. They contribute essentially to non-availabilities of hydrogen refuelling stations. Getting rid of dedicated compressors will reduce investment costs and improve availabilities besides the gain in efficiency provided by the high pressure electrolysis.
In order to optimize the process of high pressure electrolysis, the knowledge about the behaviour of bubbles at high pressure has to be improved. Therefore a model for the simulation of the bubbles at high pressures is developed at the IKET. The electrolyser cell with the optical access is made to achieve data about the two-phase transport of the gas in bubbles in the electrolyte. This data is necessary to implement into the developed model.

2.2 Behaviour of Hydrogen Gas Bubbles under high pressure

2.2.1 Stages of the bubbles

A study of the behaviour of hydrogen gas bubbles under high pressure results will be carried out in this section. The production of electrolytic hydrogen involves two gas evolution processes, of hydrogen itself and oxygen, as seen in the eqs. (2.1) to (2.3) before. The kinetics of these reactions is dependent on the complex electrochemical and three phase physics of the evolved gases on the electrode and in the electrolyte.
Three main stages can be identified on the bubbles' evolution: nucleation, growth and detachment. Bubbles start nucleating at electrode surface from an advanced solution process once it becomes highly supersaturated. Bubbles grow by dissolved gas diffusion to their surface or by coalescence with other bubbles, and finally they detach from the electrode when the forces pulling them away supersede the attractive forces. The key stages of the gas bubbles evolution, which has been derived and evaluated only for ambient pressure so far, will be explained in detail in the following.

Bubble nucleation

The first phase called nucleation takes place when the electrolyte near the electrode is supersaturated with produced gas, as stated before. A flux of H_2 based on a current density of a few milliamperes per square centimetre (mA/cm^2) is sufficient to supersaturate the liquid, since H_2 is sparely soluble. When the dissolved gas concentration reaches a critical value, bubbles nucleate and grow. This critical value can be calculated from the classical nucleation theory, according to Sequeira [5].
According to the classical nucleation theory, density fluctuations produce vapour nuclei that may grow or decay depending on whether the bubble nucleus is higher or smaller than a certain size, determined by so-called critical radius (or diameter). At this stage, the bubble is in metastable chemical and mechanical equilibrium with its surroundings. Therefore, "the essential features of nucleation theory are the expression defining the size of the critical bubble nucleus and the formulation of the rate expression as an exponential function of the work associated with the production of a nucleus having

this dimension" defines Sequeira [5].
An expression for the critical radius for multicomponent systems was found by Ward[6]:

$$R_c = \frac{2\sigma}{\frac{\eta \cdot P_\infty}{\nu_1} + \frac{P' \cdot C'}{\nu_2 \cdot \underline{c}_0} - P'} \tag{2.8}$$

where P_∞ is the vapour pressure of solvent at the temperature of the liquid; P' is the external pressure in the liquid; ν_1, ν_2 are the vapour phase activity coefficients of the solvent and solute; C' is the concentration of the gas in the solution surrounding the bubble, expressed as moles of solute per mole of solvent; $\underline{c}_0$ is the equilibrium concentration of the gas in the solvent when a flat surface of the solvent is exposed to the gas only at T' and P', expressed as moles of solute per mole of solvent; σ is the surface tension of the liquid–gas interface often assumed equal to the surface tension of the liquid vapour interface; and η is defined as:

$$\eta = exp\left(\frac{V_1(P' - P_\infty)}{kT}\right) \tag{2.9}$$

Where V_1 is the specific volume of the pure solvent.

Bubble growth

The growth of gas bubble is caused by the continuous diffusion of dissolved gas to the gas/liquid interface and the coalescence of bubbles. Several studies were performed to understand this bubble stage. A first square-root-of-time growth dependence was confirmed in the works of Scriven [7] and Westerheide and Westwater [8] for a single bubble. This could not be applied to multiple bubbles due to interference. However, it could be concluded that the initial mechanism of bubble growth happens by diffusion of gas to the bubble surface. The diffusion-limited initial stage of growth being established, the significance of coalescence in the next stage was pointed out. As stated by Janssen and von Stralen [9] when exploring O_2 bubbles evolution in aqueous potassium hydroxide (KOH) on a transparent nickel (Ni) electrode, frequent coalescence was found, followed by mobility of bubbles on the electrode surface, and a radial movement of small bubbles toward large ones and "consumption" of small bubbles by large ones at high current density.

Bubble detachment

Detachment as the final phase in the physics of bubbles evolution has also been the subject of both theoretical and experimental studies. The bubbles are found to detach once the surface adhesive forces, related to bubble contact angles, can no longer restrain them. Following the studies of Zhang and Zeng [4], a force balance analysis around an electrolytic bubble is performed based on two types of electrolytic gas evolution models. For the present work only the stagnant model will be described, as it helps to understand better the forces balance. Figure (2.2) shows a basic model of the forces' balance.

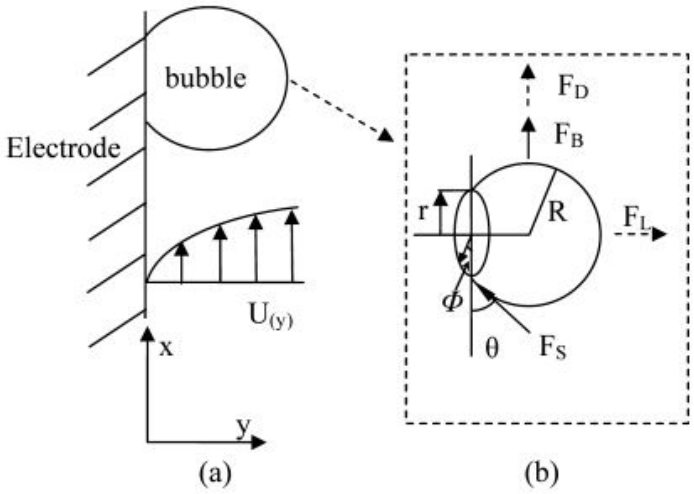

Figure 2.2: Schematic diagram of a gas bubble on an electrode surface (a) and the forces acting on the bubble (b) [4]

The x coordinate is in the oposite direction of gravity, and the y coordinate is normal to the x coordinate, pointing outward from the electrode, respectively. The electrolyte flows in the direction of the x coordinate. Buoyancy and surface tension exist due to the density difference between liquid and gas and the property of the solution, respectively. In the presence of the electrolyte flow, a drag force and a lift force also come into play. As stated by Zhang and Zeng [4], the force incurred by the temperature field effect is neglected by maintaining the temperature of the electrolyte constant. The forces acting on a gas bubble can be decomposed into components along both suggested coordinates, resulting in possible movements of gas bubbles in the corresponding directions. These movements will be called as departure and lift-off.

The buoyancy F_B is composed of the force from the pressure and the gravity on the mass of the gas bubble. Due to the growth of the gas bubble with the gas production, the pressure of the bubble experiences a dynamic change, represented by the expansion force F_G. This force is not shown in figure (2.2).
The inter-facial tension force F_S exerted on the gas bubble exists along the circular contact line where the gas, liquid, and solid phases are in contact with each other. The surface tension and the contact angle are the two key components determining the inter-facial tension force. Throughout different empirical studies, the surface tension can be found as a function of the electrolyte concentration gradient, pressure gradient, temperature gradient, and voltage gradient, respectively. When the gas bubble is attached to the electrode surface as shown in figure (2.2), both static force and balance conditions $\sum F_x = 0$ and $\sum F_y = 0$ are satisfied. Once one of these conditions is broken, the gas bubble departs or lifts off from the electrode, causing the detachment.
In the stagnant model, when the gas bubble attaches on the electrode surface, $\sum F_x = \sum F_b > 0$. Therefore, the buoyancy force is not balanced with the sum of the other forces. This unbalance will force the bubble to tilt upward to reach a new force balance and then departs when the bubble can no longer tilt after sufficient growth in size. The upward tilting of the bubble causes so-called advancing and receding angles, causing an inter-facial tension force in the x direction, which balances with the buoyancy force to maintain the bubble temporarily attached to the electrode.
In addition, it can be predicted that varying the electrolyte concentration and the electrode potential will alter the inter-facial tension force and thus the critical diameter for the bubble departure. This will be further discussed on the subsection 2.2.3.

2.2.2 Operating parameters

Smaller gas covered electrode surface and smaller bubble diameter reduce the effective resistance and thereby increase the electrolysis efficiency.
The final size of the bubbles is determined by several parameters including electrode material, current density and different additives. Although, it has been established that current density affects bubble size, there are still some disagreements in the literature about its exact effect. Several studies e.g. [10] showed that the presence of different additives in the electrolyte solutions results in evolution of smaller bubbles in most cases with formation of foamy mixture being observed. The effect of these additives

relies on reducing the ratio of bubble/contact diameter by about half of it and therefore increasing the wettability of the electrode. Nevertheless, the forces holding the bubbles to the electrode were most likely weakened proportionally to the decrease of both the perimeter of the contact area and the contact angle. Moreover, it is believed that the presence of inhibitors stabilizes the bubble interfaces and averts their coalescence on the electrode. Moreover, current density value and presence of additives in the electrolyte, other process parameters have been reported to influence bubble size and behaviour. For instance, the next figure shows the critical diameter of the bubble as a function of the current density in a sample solution [11].

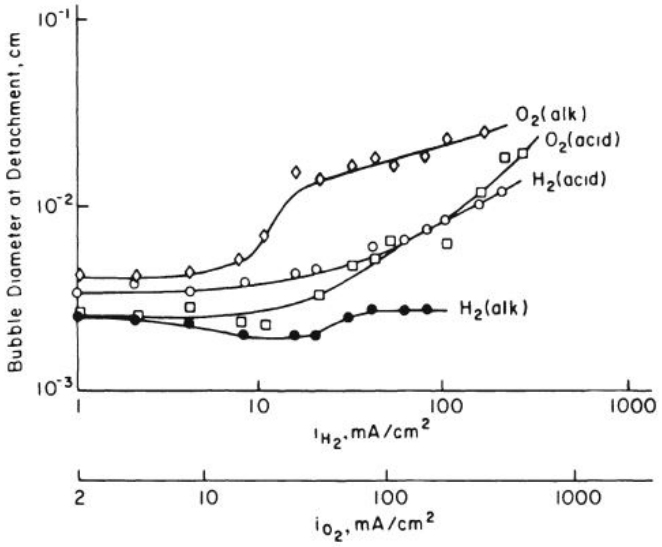

Figure 2.3: Bubble breakoff diameter as a function of current density for an horizontal Pt gas-evolving electrode in various solutions. [5]

It can be easily identified that all bubbles besides H_2 in alkaline solution increased with a raise in the current density, due to more frequent coalescence of bubbles. On the other hand, some authors (Venezel [10]) have studied and concluded a contrary effect on the current density. Still there are some disagreements on this topic.
Furthermore, electrode orientation and configuration are also expected to affect bubble size. The conductivity of a heterogeneous medium, an important topic in diverse technical problems, depends on three characteristics: the ratio of the conductivity of the dispersed and continuous phases, the gross volume fraction occupied by the dispersed phase, and its state of aggregation. Depending on whether its conductivity is greater or lesser than the surrounding medium, the dispersed phase can enhance or slow down transport.

2.2.3 Influence of bubbles' critical diameter

The critical diameter of the bubbles is influenced by the variation of the electrolysis conditions, as it was analysed before. In this subsection, a summary of the results obtained will be discussed, according to the carried out studies by Zhang and Zeng[4]. The critical diameter for hydrogen bubble departure increased with increasing current density. The trend of increasing the critical diameters with increasing cell voltage can be explained by the increased inter-facial tension at higher electrode potentials. At a higher current density, the cell voltage was also higher and therefore the inter-facial tension force in the x coordinate direction was greater. Furthermore, the bubble buoyancy force had to be large enough to overcome the inter-facial tension force by increasing the bubble diameter.

The electrolyte concentration also plays an important role in the inter-facial force. Therefore, the study of its effect on the critical diameter for bubble departure must be also performed. It was found that increasing the KOH concentration from 0.5 to 4 M dramatically decreased the critical diameter for hydrogen bubble departure and the number of bubbles was reduced as well. A similar decrease in the critical diameter was also found for the oxygen bubbles. The increase in viscosity results in an adverse effect. It is thought that the change in viscosity led to the decrease in contact angle difference between the bubble and the electrode (referred as $\Delta\theta$). The increased viscosity made it harder for the bubble to tilt or stretch, which would result in the decrease of the contact angle difference $\Delta\theta$.

As can be easily seen, the diameter of the largest bubble departing the electrode was drastically reduced as expected when the electrolyte circulation was applied due to the drag and lift forces of the bubble-enhanced convention. The application of the electrolyte circulation reduced the critical diameter for departure as the circulation velocity increased. However, the bubble curtain was still on the surface of the electrode which still posed a resistance barrier for water electrolysis.

3 Design of Experimental Set Up

3.1 Construction of Electrolyser

The optical electrolyser experiment is designed to operate at a working pressure of up to $45MPa$. To guarantee a safe operation and a sufficient margin the design has been made to resist a static pressure of even $75MPa$. To observe the complex process during electrolysis, the cylindrical electrolyser is closed with partially transparent covers with glass elements. This, in fact complicates the construction of the device.
Besides the glass windows to observe bubbles' behaviour and the working pressure of $45MPa$, requirements have been made to insert different electrodes. They have to be easily exchangeable in shape, material and their distance to each other.
Figure 3.1 shows the schematic set-up of the experiment. In the figure 4.1 the complete device is shown mounted on the support plate. In this section all components of the set-up and their functions are briefly introduced. Their design is described in detail in following sections.

In order to pressurize the system with nitrogen, a bottle of high pressure nitrogen is to be connected to the passing valve, which is linked to the main cylinder of the optical electrolyser. A manometer measures the total pressure on the system and the safety valve ensures the pressure does not exceed the limit of $45MPa$. On the other side of the elecrolyzer the secondary separation tank and the manual pump are connected to the system. The secondary tank leads to two separated circuits. The first one is connected to the main tank, filled with the electrolyte, during the described experiments potassium hydroxide has been used exclusively for this purpose. The second circuit is filled with hydraulic oil and connected to the manual pump. A piston inside the tank separates two liquids. In order to fill the main tank with potassium hydroxide and to raise the pressure to a level above the pressure of the nitrogen tank, the piston inside the separation tank has to be moved towards the electrolyte circuit by operating the

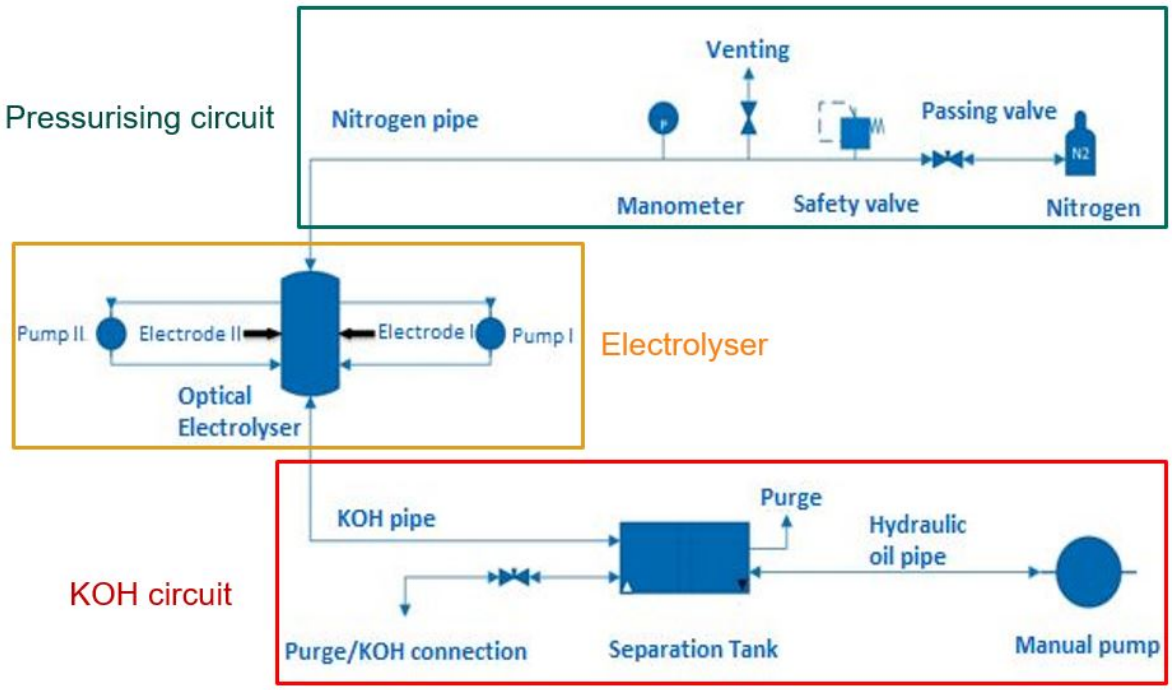

Figure 3.1: Schematic set-up

manual pump.
Furthermore the two electrodes are mounted in the main cylinder. Besides the electrodes, the nitrogen and electrolyte pipes and two circulation pumps are connected to the main cylinder. The pumps are required to circulate the electrolyte in order to achieve a forced flow at the electrodes. However, the pumps are not required for the first series of experiments but may be of interest for further research. The external pumps are laid out for a maximum pressure of $200bar$. When operating the system at higher pressures the pumps have to be disconnected and the respective screwed connections in the main tank have to be closed by blind fittings!

3.1.1 Main Cylinders

Both main cylinders, the cylindrical of the optical electrolyser cell, as well as the one of the separation tank are built from the same raw material. The cylindrical tubes are made of SAE 1020 steel with an outer diameter of $114mm$ and in inner diameter of $83mm$. The corresponding wall thickness is $15.5mm$.
The sufficient dimensioning of the tanks are calculated with the pipe formula shown in eqs. (3.1) and (3.2). Where σ_t is the tangential stress and σ_a the stress in the axial direction, p is the pressure, d_m the mean diameter and s the thickness of the wall.

$$\sigma_t = \frac{p \cdot d_m}{2 \cdot s} \tag{3.1}$$

$$\sigma_a = \frac{p \cdot d_m}{4 \cdot s} \tag{3.2}$$

Main tank

The main tank of the optical electrolyser contains eight UNF 9/16–18 threaded holes in the outer wall. They are arranged in two circles of four holes each. A threaded UNF 9/16-18 diameter was chosen in order to use standard fittings for ¼-inch tubing. The electrodes as well are designed in such way that they are compatible with the fittings. This allows to vary the arrangement of the input pipes and electrodes into the cylinder individually for the requirements of each experimental set-up. The length of the cylinder is $85mm$ which makes a resulting inner volume of the device usable for the electrolysis of $460cm^3$.

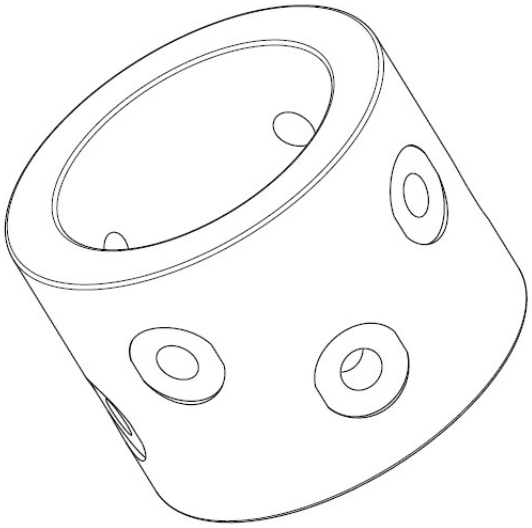

Figure 3.2: Cylindrical Main Tank

Separation tank

For the experiments with higher pressure than the $200bar$ of the N_2 storage pressure, it is necessary to rise the pressure by a separate pump operating with hydraulic oil. It is essential that the hydraulic oil circuit and the circuit of the electrolyte do not mix. Therefore, the separation tank is required as a storage of hydraulic oil and electrolyte at the same time. Equipped with a piston to reliably achieve the isolation of the fluids and to push or release the electrolyte into the tank.
The separation tank possesses the same net inner volume than the main cylinder in order to assure that even if the electrolyser is empty at the initiation of the experiment, it can be completely filled with electrolyte stored in the separation tank and the desired working pressure can be reached.
On both sides of the tank, the electrolyte and the hydraulic oil circuit, a valve is included for the purpose of ventilation.

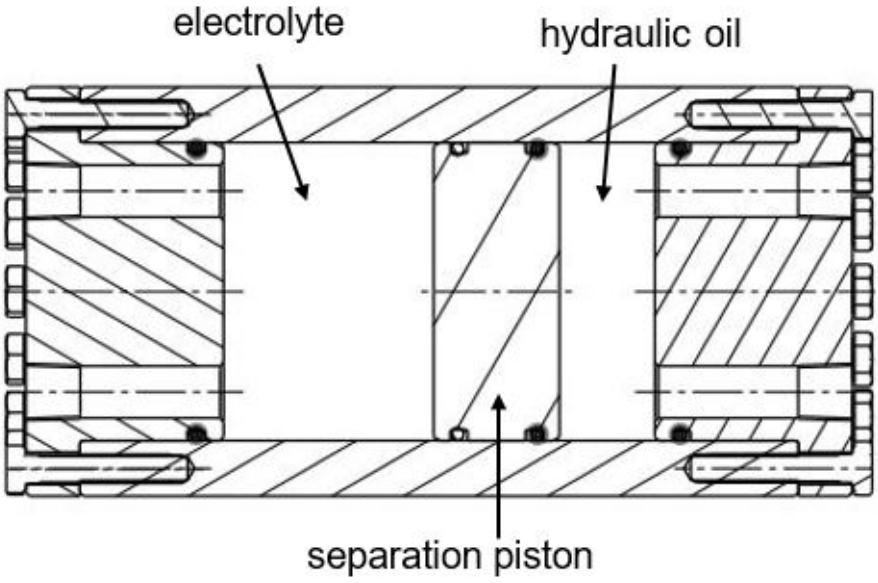

Figure 3.3: Separation Tank with piston

3.1.2 Top Cover and Glass Lid

As one the main ideas of the project is the visualization of production and behaviour of the gas bubbles under varying pressures, the way of implementing the glass windows into the electrolyser is a fundamental design task.
The most critical component is supported by the metal frame of the top cover, which is adjusted to the design of the window which is made from borosilicate glass. A maximum hydraulic pressure of $75MPa$ has to be resistible. For calculations of the design an additional safety factor of nearly 2 at maximum load has been obtained. During all stages of design and construction of the top covers, the results have been simulated with finite element method (FEM) by the hydrogen group of ITBA university using the software $ANSYS$.
Analyses have shown that conical shaped glass instead of a cylindrical, allows a significant reduce of the thickness in order to achieve the required factor of safety. The most committed point is in the top center of the borosilicate glass (see fig.3.4), which possesses a limit of maximum stain of $\sigma_T = 50MPa$. The maximum strain impacting on this point at a pressure of $750MPa$ is $\sigma_{r,max} = 25.6MPa$. The maximum deformation calculated is $y_{max} = 0.029mm$.
The finally obtained shape is a conical glass with an angle of 35° and a thickness of $25mm$.

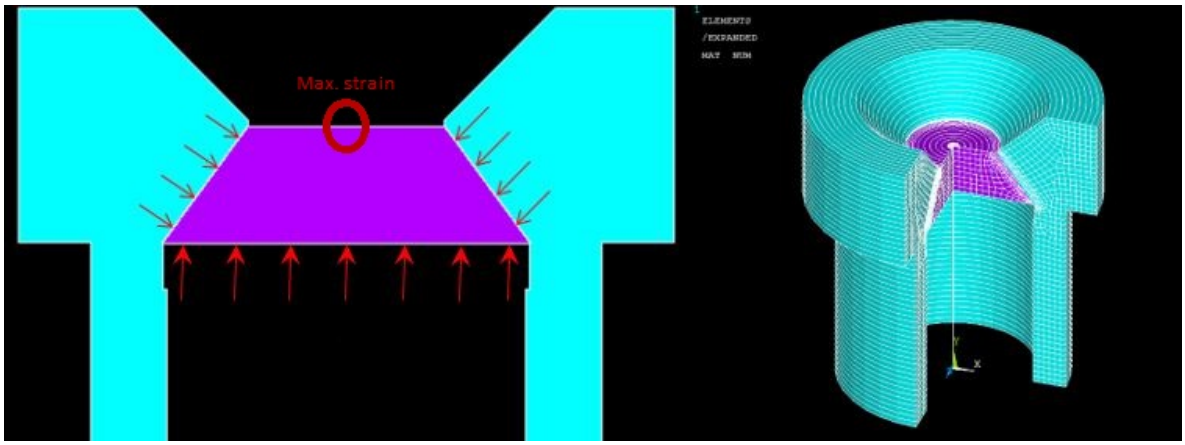

Figure 3.4: Design of the Taps and window element

Between the glass and the metal frame of the top cover a plastic interface is added. Advantages of this plastic layer, which is made out of epoxy raisin, are the dissipation of stress which may occur due to surface imperfections in the structured parts caused

by the respective fabrication process. This way local stress peaks are avoided and a sealing function is provided.
Various series of experiments with different types of resin epoxy have been made to guarantee that the material resists the design and test pressure respectively. Another aspect is the cycling stability of the plastic interface.
Results of the compression experiments with raisin epoxy are illustrated in figure (3.5). Deformation of the epoxy probe during the compression and the subsequent release are depicted.

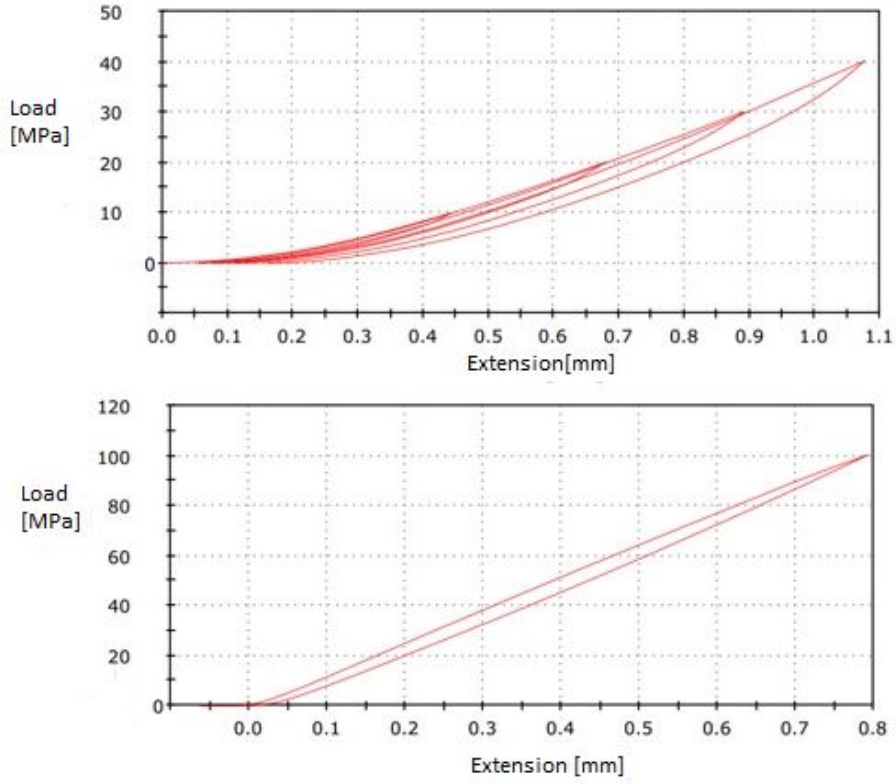

Figure 3.5: Compression experiment of Resin Epoxy

Figure (3.6) shows the final assembled main tank. Screwed top cover and glass windows.

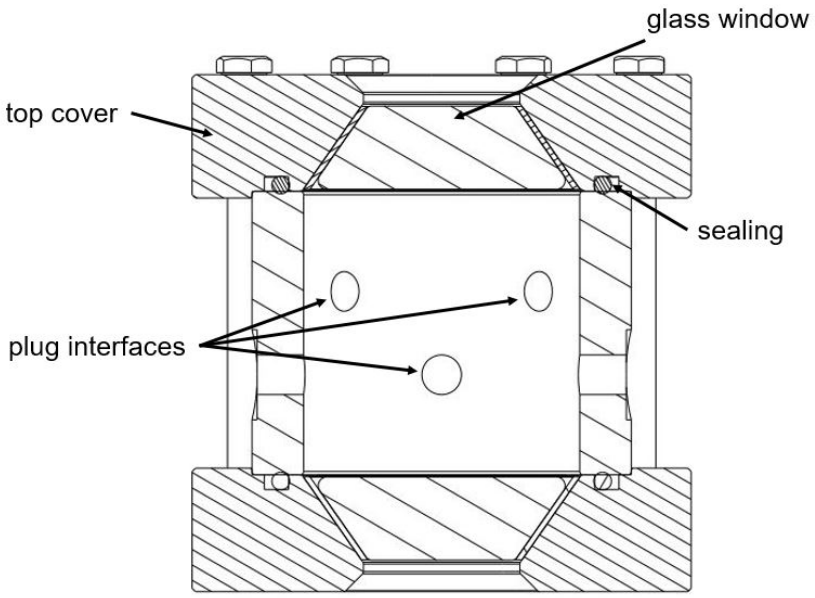

Figure 3.6: Main tank with top cover and glass windows

3.1.3 Pressure Generation

For the pressure generation the first step is to pressurise the system by the connected nitrogen bottle normally up to 200*bar* or 300*bar*, depending on the nitrogen source. Higher working pressures are achieved using the manual pump and the separation tank. As mentioned before the separation tank divides the electrolyte circuit and the hydraulic oil circuit by a piston. By operating the manual pump which has a limit of 700*bar* the piston is pushed towards the electrolyte circuit. This has two functions. Liquid is being pumped into the optical electrolyser tank and an increase of pressure in the system is caused.

If at the start of the experiment the main tank of the electolyser is filled with nitrogen and as second step the electrolyte is pumped into the tank until half of the volume is filled by incompressible liquid the resulting pressure can be calculated. At working pressures up to 100*bar* the compressed nitrogen can be assumed to be a ideal gas and the resulting pressure can easily be calculated using eq.(3.3).

$$p \cdot V = n \cdot R \cdot T \tag{3.3}$$

As n, the number of moles of the compressed gas, the universal gas constant $R = (8.314\frac{J}{mol \cdot K})$ and the Temperature T are constant, the pressure change depends only on the change of volume.

$$\frac{p_1}{p_2} = \frac{V_2}{V_1} \tag{3.4}$$

Compressing the nitrogen at temperatures arround 20-25 °C in the system above $100bar$, the assumption of a ideal gas is not valid any more and the eq. (3.3) has to be expand by a term describing the real gas behaviour as it is done in the eqs. (3.5) and (3.6).

$$p \cdot V = n \cdot R \cdot T \cdot (1 + B(T) \cdot \rho + C(T) \cdot \rho^2 + D(T) \cdot \rho^3 + ...) \tag{3.5}$$

$$(1 + B(T) \cdot \rho + C(T) \cdot \rho^2 + D(T) \cdot \rho^3 + ...) = Z(T, p) \tag{3.6}$$

This factor of correction between real and ideal gas behaviour is the compressibility factor Z. It depends on the the pressure and the temperature. As the electrolyser operates at temperatures between about 20°C to 25°C and the variation on Z due to the change of temperature at this range is insignificant, the temperature is seen as constant. Eq. (3.4) has been adapted to real gas behaviour and the pressure necessary to pre compress the system is calculated using eq. (3.8).

$$p \cdot V = n \cdot R \cdot T \cdot Z(p) \tag{3.7}$$

$$\frac{p_1}{p_2} = \frac{V_2}{V_1}\frac{Z_1(p_1)}{Z_2(p_2)} \tag{3.8}$$

Figure (3.7) shows the evolution of the compressibility factor Z of nitrogen at the temperature and varying pressures. It shows that the difference between a real gas behaviour and a ideal gas behaviour increases significantly at rising pressures. Up to $100bar$ Z is almost 1 and therefore real gas properties of nitrogen can be neglected.

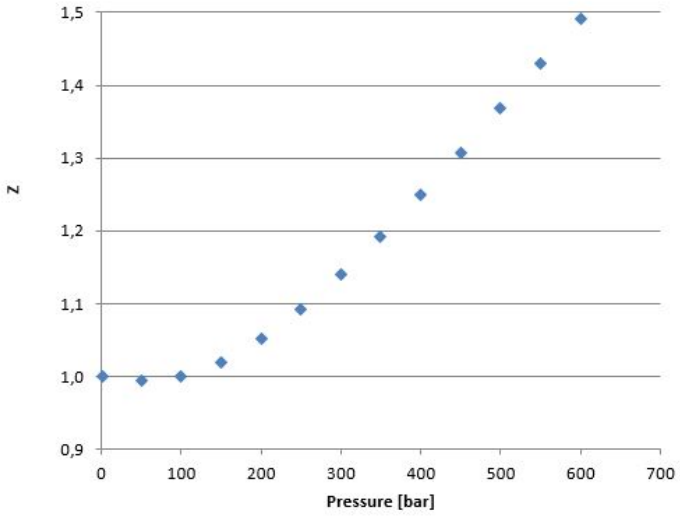

Figure 3.7: Compressibility factor $Z(nitrogen, 20°\mathrm{C})$

At the beginning of the process the main tank has no electrolyte and is being pre-pressurised with nitrogen to the pressure p_1. Compressing electrolyte into the tank until half of the tank is filled a new pressure p_2 is reached. Operating the system, usually p_2 is known as the working pressure for the execution of the experiments. The required level of pre-pressurisation p_1 has been calculated eq. (3.8) and is shown in table (3.1).

Table 3.1: Pre-pressurise tank

$p_2[bar]$	25	50	75	100	125	150	175	200	225	250	275	300	325	350	375	400	425	450
$p_1[bar]$	13	25	37	49	60	73	84	95	106	116	126	136	146	155	163	171	179	186

3.1.4 Electrodes

The electrodes are the central parts of the electrolyser cell. During the process of designing them attention has been turned on fulfilling various functions. The electrodes are screwed into the provided holes in the cylinder of the main tank. The thread is a UNF 9/16-18 as the fittings, to enable that the electrodes can be plugged in any of the eight holes in the cylinder. O-ring seals prevent leakage from the tank, even at the high operation pressures.

The main function of the electrodes is to conduct the direct current to their tips. All other components have to be electrically isolated to prevent electrical charge or current on the cylinder tank or any other parts.
This isolation has been achieved by covering the electrodes with a non conductive material. The plastic PEEK was chosen because it shows excellent properties in rigidity to stand the required forces caused by the high pressure and its good properties with regard to machining. Figure 3.8 shows the design of the assembled electrode. The parts shown in transparent brown color is the PEEK isolator covering the shaft of the electrode. The shaft is produced from stainless steel with a diameter of $4mm$ and a length of $75mm$. Both ends are threaded, one side has a $4mm$ thread in order to be screwed into the tip of the electrode. The other side is threaded $10mm$ to attach the electric power supply to the electrode.

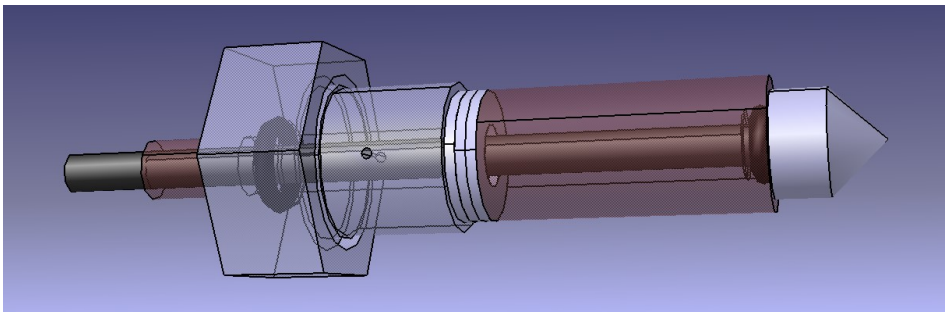

Figure 3.8: Assembled Electrode

The reason for connecting the tip and the electrode shaft by a screw is to assure an easy replacement of the tips. In figure 3.8 the electrode is equipped with a cone shaped tip. During first experiments various different geometries have been tested. Depending on the aim of the experiment and the geometry of the electrode tips, it might be of interest to vary the distance of the electrodes to each other. For this purpose shims which are located between the PEEK and the screw can be added or removed.

Further studies of electrodes with quadratic tips and a membrane to separate the oxygen and the hydrogen have been made. For the later case a transparent acrylic box has been developed in which the electrodes and the membrane are placed. This way a confined space is provided for the electrolysis which mimics the condition in a real electrolyser stack. Chapter 4.2.2 describes the electrode shape actually applied in the reference experiments.

3.2 Optical Measurement Instrumentation

3.2.1 Bubble diameter measurement

Laser and CDD Camera

The set-up for the laser and the CCD camera unit requires more space than the standard camera. The set-up of the system can be observed in figure (3.9).

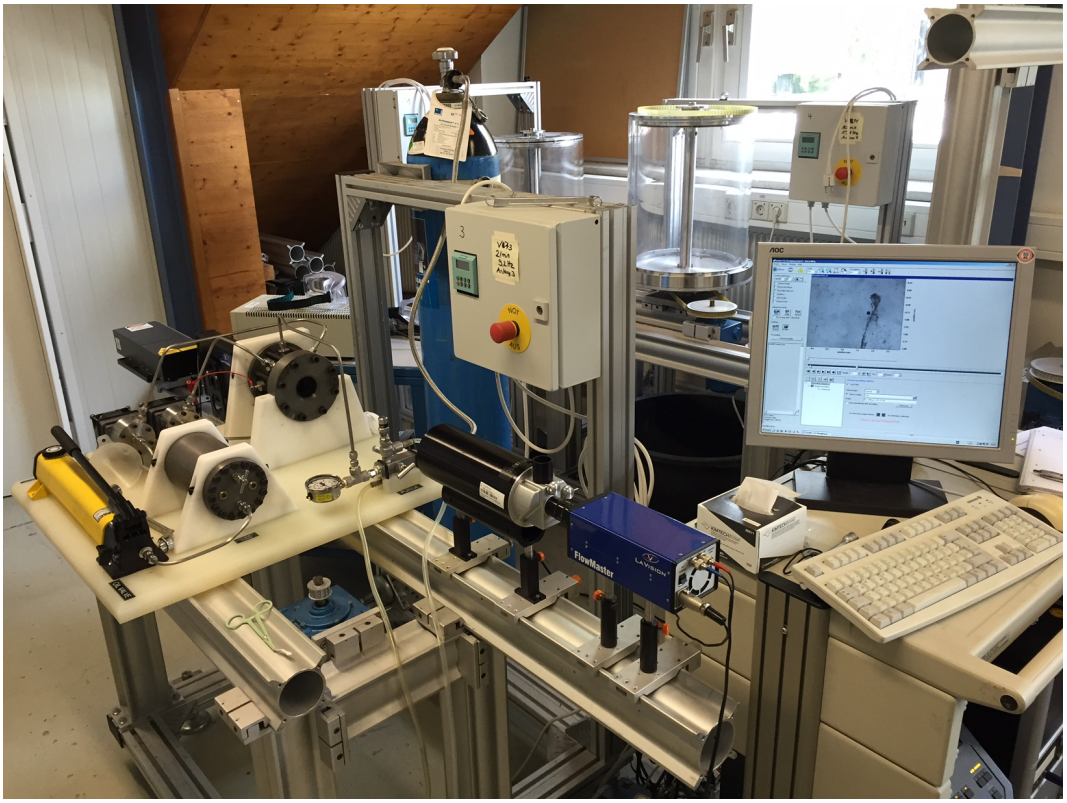

Figure 3.9: Set-up Laser and CDD Camera

The laser and the camera are connected to the computer which triggers the laser impulse and the regulates the camera. The picture taken by the CDD Camera can directly been observed on the connected screen. Adjustments in the sharpness of the picture can be realized by moving the device on the optical axis into the focus.

Laser with long distance microscope

For measuring the expected small size of the gas bubbles a double-pulsing-Nd:YAG laser with a weave length of $532nm$ is used. The laser beam is led special optics in a coaxial parallel direction. This ensures that in the observation field each bubble is illuminated in the same way. The frame rate can be adjusted between 0.5 and 3 frames per second. Next to the laser a diffuser is installed (Fig. 3.10). Inside the diffuser the laser beams are lead though a glass sheet, which is endowed with fluorescent pigments. The fluorescent light of the glass shield is led by mirrors into the head of the diffuser, where it is being expanded to a homogeneous illumination. The scatter window of the diffuser has a diameter of $120mm$.

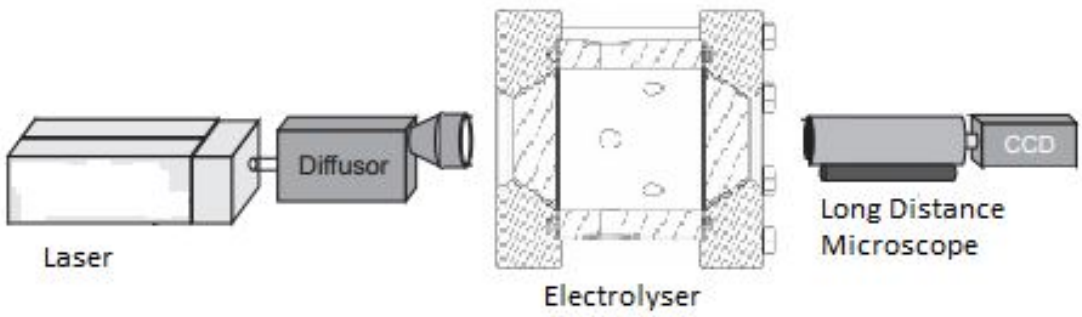

Figure 3.10: Set-up laser

For the experiments the position of the diffuser is adjusted in such way to the electrolyser, that the illumination inside the tank is homogeneous and can be adjusted in intensity. On the opposite side of the electrolyser cell the camera is installed in a collinear way on the same axis.
For capturing the images a CCD-Camera (Charge Coupled Device) with a resolution of 1280 x 1024 Pixel is being used (FlowMaster 3S, LaVision). A long distance microscope is placed ahead of the camera (Fig. 3.10), in order to achieve a high depth of sharpness in the observation window. The distance between the long distance microscope and the tips of the electrodes in the electrolyser is $56cm$. The camera system is calibrated with calibration sheet before starting operation. The resolution of the camera counts $2.5\mu m/pixel$. The observation window of the camera is $3.17mm$ wide and $2.52mm$ high. A computer is connected to the system in order to control the trigger of the laser and

to capture the data of the camera. The pulse of the laser takes between $5 - 7ns$. For each measurement campaign unit 50 pictures are taken with a trigger rate of 3 pictures per second.

Evaluation of the pictures

For the evaluation of the images taken CCD-Camera the software *ImageJ* is being used. *ImageJ* is a Java based open source program designed for medical and scientific picture analysis especially. After loading the pictures into the program first of all the scale has to be set. In a second step a global threshold has to be set. The global threshold defines a minimum intensity of gray scale level, which the bubbles' images have to provide in order to be recognized as bubbles by the software. As it is shown in figure 3.11, only elements which exceed the global threshold are recognized and their dimensions are determined. The threshold has to be adjusted for each sequence depending on the illumination intensity and contrast.

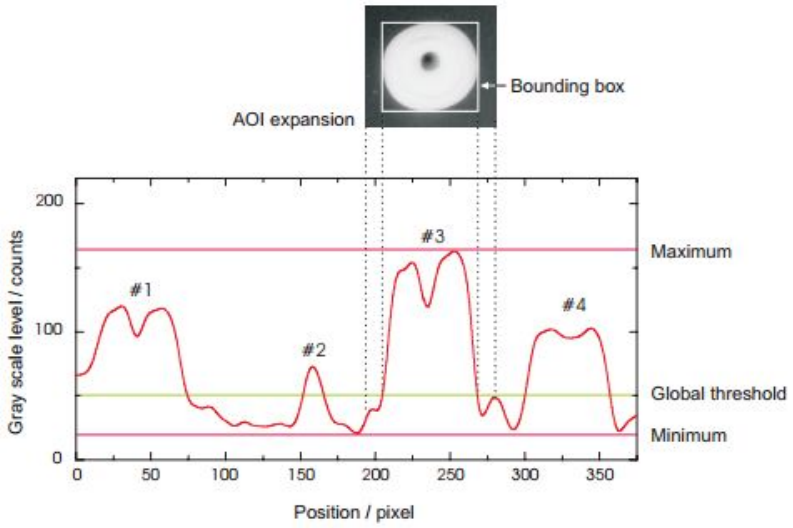

Figure 3.11: Threshold setting for analysed bubbles [13]

After adjusting the global threshold, the bubbles can be analysed. *ImageJ* provides an option for this matter. As the rising gas bubbles often stick together to a form cloud of bubbles it is not possible for the program to detect every single one. It is possible to set a minimum circularity of the particles. That means if various bubbles are sticking together software recognizes them as one big particle which does not provide the required circularity and then excludes them from further processing.

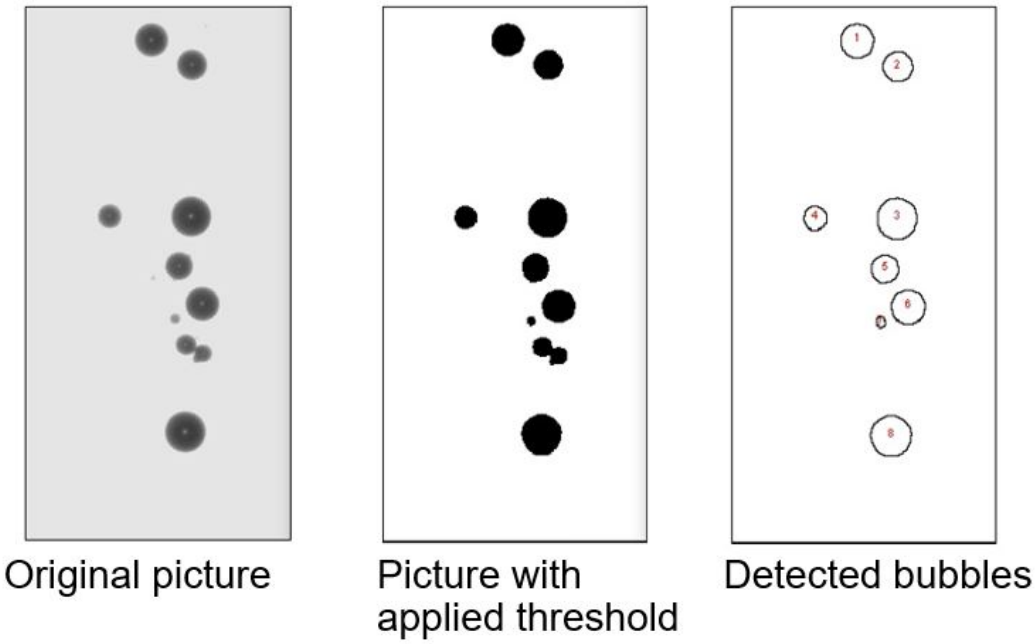

Figure 3.12: Atomised post-processing of the raw images

Figure 3.12 shows the steps of evaluating the particles. The original picture taken by the CCD camera; Followed by the same picture with the applied threshold, the grey-scale is set and possible image noise is subtracted; The rights picture shows the detected analysed bubbles which full fill the required circularity of 80 % between minimum and maximum diameter. In this case two bubbles are not taken into account, because the program does not detect them as two separate particles.
With the help of the registered bubbles statistics about diameter distribution and mean diameter can be made.

3.2.2 Velocity determination of the bubbles

Panasonic HC-V500

For the experiments measuring the rising velocity of the gas bubbles, the Panasonic HC-V500 is placed in front of the glass window of the main tank as it can bee observed in figure (3.13). The tips of the electrodes have to be included on the picture in order to serve as a reference in the following evaluation.
A white sheet is put on the opposite window for illumination.

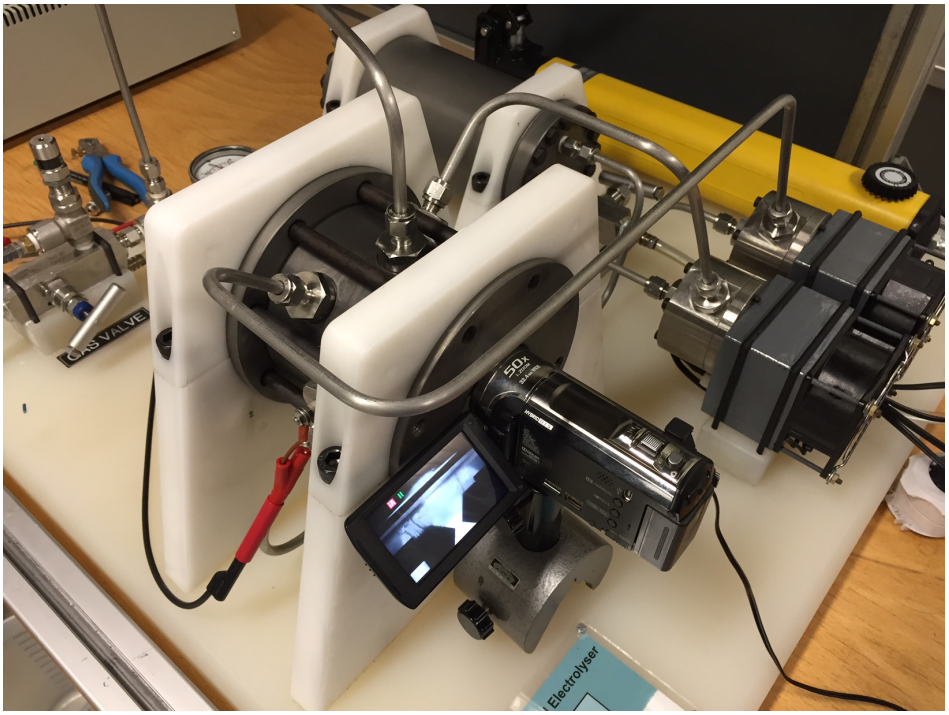

Figure 3.13: Set-up Panasonic HC-V500

Buoyant Velocity

In order to evaluate the rising velocity of the oxygen and hydrogen bubbles a standard digital movie camera which takes 50 pictures/second with a resolution of $1920x1080$ pixels is used. Therefore a stack of pictures at one determined pressure is analysed.

Assuming a constant raising velocity and knowing the lapse of time between the analysed frames, the rising velocity can be calculated by a simple trigonometric equation.

$$tan\alpha = c = \frac{\Delta h}{\Delta t} \tag{3.9}$$

As it is shown in figure 3.14 by the adjacent leg dt the time is determined, the stack of bubbles requires to cover the distance dh. The measurement equipment, in particular the resolution of the camera does not allow the analysis of single bubbles but only the cloud of particles. The mean diameter of the bubble cloud at a given pressure is determined in chapter 5.1.
The buoyant velocity is analysed for hydrogen such oxygen at pressures between $1bar$ and $150bar$.

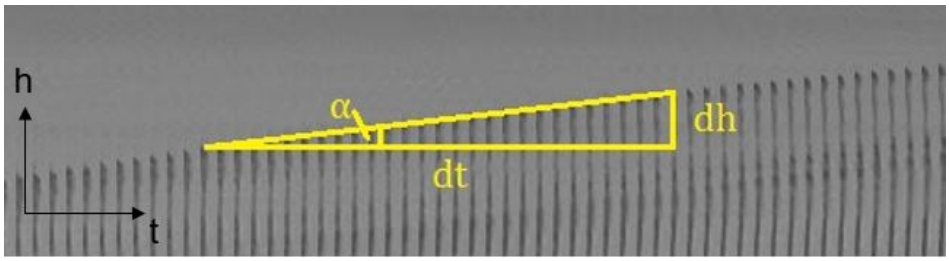

Figure 3.14: Determination of rising velocity

3.3 Analysis of error

The error in the measurement of the bubble diameter depends on the local resolution of the camera such as the size of the detected particle. Pfeifer used the same installation as described in chapter 3.2.1, *bubble diameter*. According to his analysis a single droplet with the diameter of $d_D = 6\mu m$ shows an uncertainty of 20%. For a sample of droplets this uncertainty has no influence on the mean diameter, but only on higher statistical moments (variance etc.). The uncertainty of a single bubble with the diameter of $d_D = 50\mu m$ is 3%. Therefore a global incertitude of 4% regarding the measurement of the bubbles' diameter is assumed[12].
Further studies have been made regarding the depth depth of focus. Big particles show a higher depth of focus then smaller particles. In order to detect as well small bubbles reliably, a depth sharpness of $0.5mm$ the systematic error is $\pm 0.1mm$ is estimated [12].

The probe volume is defined in two directions by the field of view of the camera. Only particles which are completely inside this field of view can be evaluated appropriately. The probability that large particles are completely inside this area is smaller compared to particles of smaller sizes (Fig. 3.15). Following function takes into account the probability $p_{i,Border}$ of bubbles entering the field of view completely.[13]:

$$p_{i,Border} = \frac{(W - D_i) \cdot (H - D_i)}{W \cdot H} \tag{3.10}$$

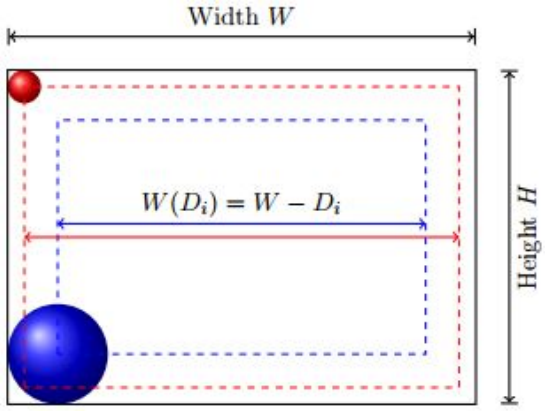

Figure 3.15: Field of view depending on particle diameter D [13].

This has to be accounted for the statistical correction of the measurements of the bubble diameters.

Furthermore, the way of counting the bubbles with the software $ImageJ$ could have influence on the results. Taking into account that for the statistics only particles of a given circularity are selected, causes that all bubbles sticking together will not contribute to the statistics. However, supposing that the creation of bubble clouds does not depend on their size, bubbles of all sizes are equally ignored by the software and the statistics of bubble size distribution is not affected.

The temperature change during the electrolysis can be neglected, although parts of the electricity required for the process to split up the water molecules is generating heat. The electrical power applied to the system is 0.2 - 0.6 W which is too small to change the temperature of the device.

The largest error in the experimental procedure is related to the pressure measurement. The pressure is manually adjusted and the reading of the barometer can be reliably done with an accuracy of $\pm 5 bar$, absolute. Additionally, the generation of gas during the process of electrolysis leads to an increase of the working pressure in the system. This makes reliable reading of the system even more difficult.

3.4 Safety Analysis

Working with high pressures and chemical products like potassium hydroxide solution, hydrogen and oxygen gas requires the compliance with several safety standards.
First of all the design and the material have to be selected appropriately, such that the electrolyser cell can stand the working pressure and resist to the used chemicals. The calculated ridgy with sufficient safety factors are described in the chapter 3.1, *Construction of Electrolyser*.
Further information regarding a safe operation with the electrolyser will be given in this paragraph.

Potassium Hydroxide Solution

Potassium hydroxide is an aqueous basic solution. It is mainly produced by the electrolysis of potassium chloride. Major areas of industrial applications besides colouring and lubricants products is the utilisation as electrolyte in accumulators.

Potassium hydroxide causes massive damages when it gets in contact with the eyes. Therefore safety eye-wear has to be worn when working with this chemical and during operation of the system. As it irritates the skin in case of contact, protective clothing and equipment has to be worn such as appropriate gloves.
For the highly undesirable case that KOH gets in touch with the eyes an eye shower should be in reach for first aid and additionally a medic has to be consulted.

In the appendix a complete safety data sheet (SDS) for potassium hydroxide is attached. Please make sure to carefully read the SDS and to full-fill safety requirements before starting the operation of the device.

Hydrogen and Oxygen

Hydrogen and Oxygen gases are not dangerous for the human body. They are neither irritative at skin contact nor cause damages in case of inhalation in small concentrations. As hydrogen is not corrosive, no special requirements to the material are necessary. Due to the very low density of 0.09 kg/m^3 at (at $0°C$ and $1bar$) it is highly volatile and the

risk of accumulation at the ground does not appear.

Nevertheless hydrogen and and oxygen are explosive at a stoichiometric mixing and at a fraction of $4\% H_2$ in the gas mixture.
A typical required energy for alkaline electrolysers is [13]:

$$4 - 4.5 kWh/Nm^3 H_2 = 4 - 4.5 Wh/Nl H_2$$

The applied electrical power at the electrolyser cell during operation varies depending on the experiment from 0.2 - $0.6W$. In case of filling the tank, which has a total volume of $0.46l$, with $0.26l$ of electrolyte solution, the remaining $0.2l$ are filled with air instead of nitrogen when starting the electrolyser. Replacing nitrogen with air is a conservative assumption. When running the system at a pressure of $100bar$, about $20 Nl N_2$ are in the gas layer. $0.8 Nl H_2$ would be necessary to reach a critical fraction of hydrogen in the gas mixture. This means that in the worst case ($4 kWh/Nm^3 H_2$ and $0.6W$) under this conditions the system can be operated for almost two hours.

In the case of completely filling the tank with electrolyte solution before starting the experiments, as soon as applying the current, a gas bubble of stoichiometric hydrogen and oxygen mixture growth at the top of the electrolyser which can react immediately. As very little amount of energy stored in the flammable gas, the potential pressure pulse of a spontaneous reaction are not able to damage the windows of the device.

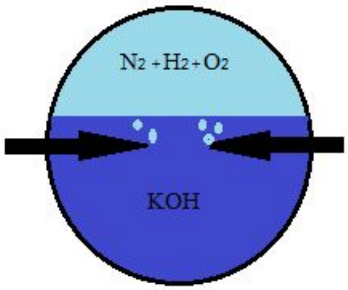

Figure 3.16: Hydrogen, oxygen and nitrogen mixture in the tank

4 Experiment Procedure

In figure 4.1 experimental set-up is shown. The subsystems as introduced in chapter 3.1, *Construction of Electrolyser* are also highlighted in figure 3.1. Only the nitrogen bottle and the power supply such as the instruments for optical measurement are not included in the figure.

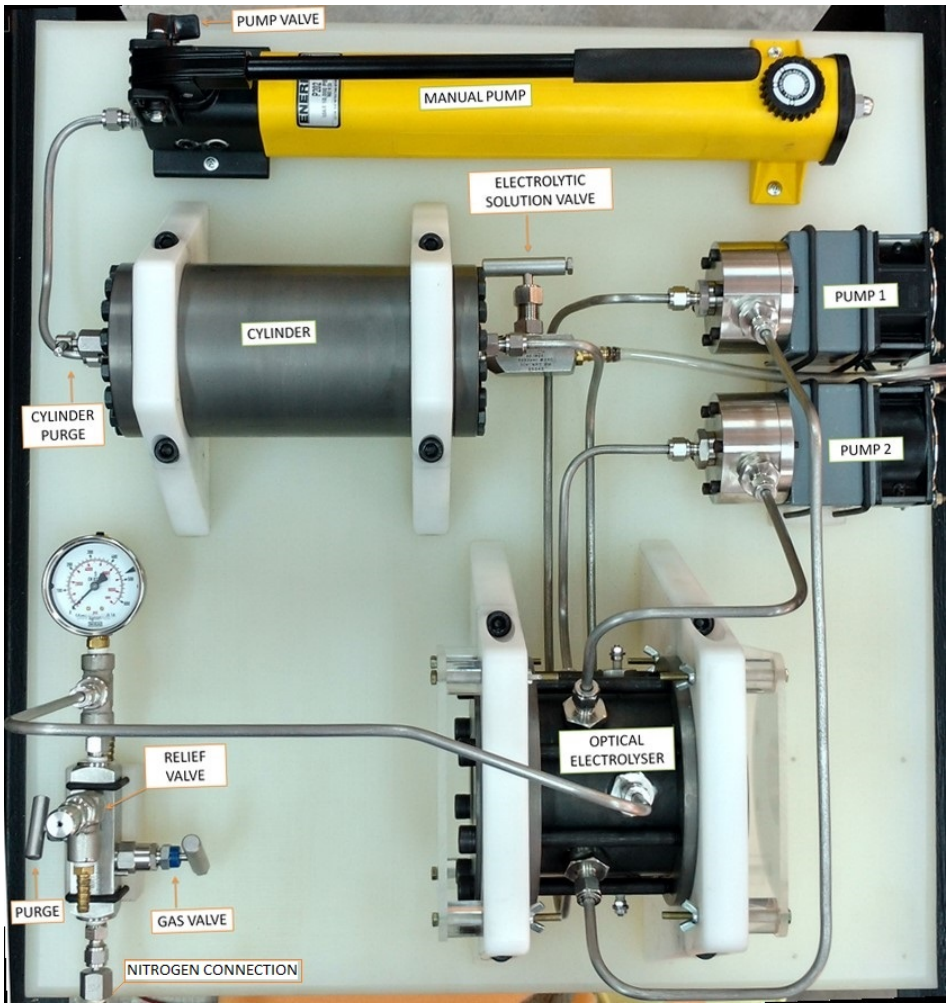

Figure 4.1: Device

4.1 Start-Up

To start up the device and run the experiments, the standard operation procedure (SOP) shell be followed, which can be found in the appendix.

A nitrogen bottle has to be connected to the system.
When operating the system at a pressure higher than $200bar$, the required safety relief valve has to be mounted which has a upper limit of $500bar$. In this case the recirculation pumps must not be connected!
When the tank has been opened, which is necessary for each change in the configuration as changing electrodes, the electrolyte has to be released before into the separation tank and the system has to be de-pressurised. When the changes in configuration have been realized and the tank is closed, it has to be ensured that leakage does not appear. For this purpose a leakage spray which detects leakages is used. The sealing has to be tested at low pressures and without electrolyte in the tank. in case of no leakage the pressure can be raised until upper safety level and tests are repeated. When the tightness of the system is ensured, the pressure can be released and the electrolyte pumped into the main tank.
Furthermore a current supply has to be connected to the electrodes to apply stabilized direct current. Typical voltages and currents are given in chapter 4.2.3.

4.2 Execution

4.2.1 Electrolyte Concentration

Potassium hydroxide is used as electrolyte during all executed experiments. The purchased solution has a concentration of $47\%vol.$. It has to be diluted to $23.5\%vol.$. Half a litre of the diluted solutions is filled into the separation tank trough the electrolyte solution valve using a provided tube and funnel. Due to contamination and sediments which lead to a cloudy recordings, the solution has to be refreshed from time to time. The solution is released via the electrolyte solution valve.

4.2.2 Shape of Electrodes

Experiments are executed with different types of electrode tips. The initially used electrodes are cone shaped ones made out of stainless steel. For analysing the bubble production with said electrode tips the shape is not convenient, because the detachment of the bubbles does not occur in one particular point as it is desired. As it can be seen in figure 4.2, the bubbles are not only produced in the very tip of the electrode and moreover move backwards along the cone, gather at the top part and detach in a undefined cloud.
The attempt to isolate the stainless steel cone except for a tiny tip and thus define the place of bubble production, does in fact focus the production location, but does not eliminate the moving along the electrode before detaching. Therefore different shapes of electrode tips are tested.

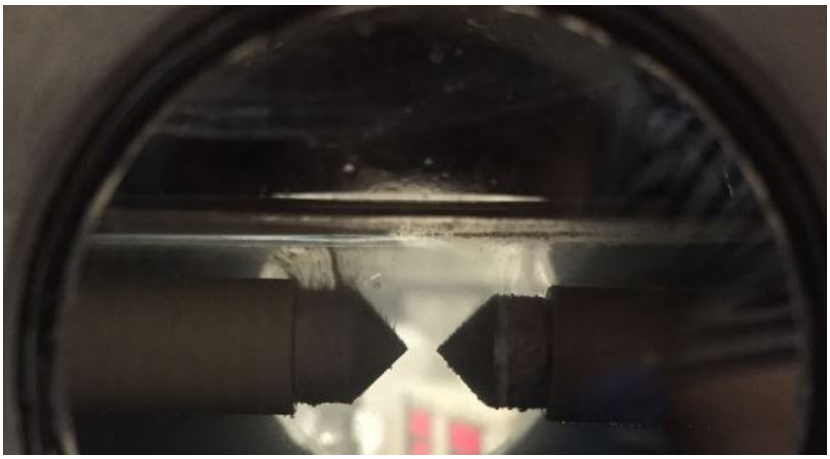

Figure 4.2: Bubble creation with cone shaped electrodes

A tip with a horizontal needle shape does improve the focusing and detachment of the bubbles at the tip. Experiments showed that the bubbles accumulate at the tip before detaching and subsequently when the first one detaches it is followed by a cloud of bubbles.

The final shape of electrode used in the experiments for the entire measurements is shown in figure 4.3. A needle shaped tip is bended in a vertical position. The tip is made out of stainless steel which is coated by paint for isolation, only the upper top is free of

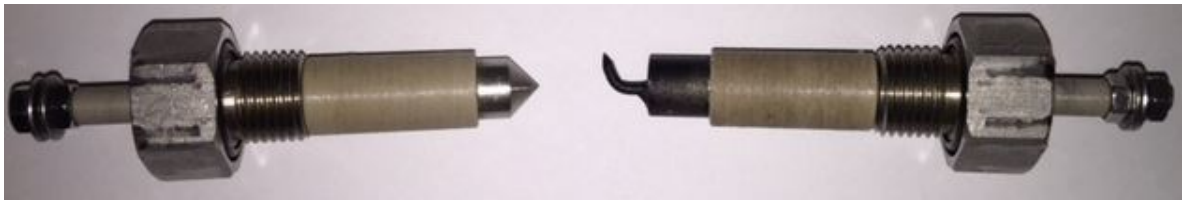

Figure 4.3: Electrode with cone shaped tip and needle shaped tip.

isolation to perform the electrolysis. This vertical shape prevents the accumulation of the bubbles before detaching and provides a localised release point for the bubbles.

4.2.3 Current/Voltage

Stabilized direct current is applied to the electrodes. The transformer utilized for the experiments has a variable adjustable voltage range between 0 - 20 V. During the analysis of the bubble behaviour voltage was set between 2.0 - 3.0 V. The current varies between 0.1 - 0.2 A depending the experiment. During one measurement series current and voltage are kept constant.

5 Reference Experiments

The test series executed are ambient pressure, $20, 50, 100$ and $150bar$. For this mean it is sufficient to pressurize the system with the nitrogen due to the nitrogen bottle reaches pressures up to $200bar$. Every experiment is executed twice, one time the oxygen producing electrode is observed and the one time the hydrogen producing electrode. This is necessary because of lack of space in the inside of the tank only one electrode is equipped with the proper vertical needle shaped electrode. The other one is equipped with the cone shaped electrode. The change from the oxygen to the hydrogen producing electrode is quickly realizable by interchanging the positive and negative connection at the outlet of the transformer.

The test series with the laser - CDD camera unit are executed in a similar way than the experiments with the $PanasonicHC - V500$. Due to the focus area of less than $3x3mm$ the adjustment of the device, laser and camera unit has to be more precisely than when operating with the normal camera without microscope. The focus area is put in such way, that the tip of the electrode appears on the lower edge of the picture taken. In this way it is ensured that all particles are captured by the camera.
Fifty pictures for each series are taken for hydrogen and oxygen separately. As the focus is adjusted precisely on one electrode tip, the poles of the transformer are interchanged in order to change from cathode to anode or vice versa.
The experiments are carried out at ambient pressure, $20, 50, 100$ and $150bar$. The manual pump is not required for this experimental set-up.

The results of the experiments, the analysis of the acquired data are presented and discussed in the following sections.

5.1 Bubble Size

The size of the rising oxygen and hydrogen bubbles are evaluated by the the software *ImageJ* analysing the pictures taken by the CDD camera. The method of analysis is described in detail in chapter 3.2. The software of the CDD camera gives as output data a list of all of all particles' areas. As the bubbles show a circularity of at least 80% the mean diameter is calculated assuming a circular area.

Hydrogen

A histogram of each measurement series is made pointing out the frequency of distribution of the diameters occurring at a constant pressure. Furthermore the mean diameter is shown.

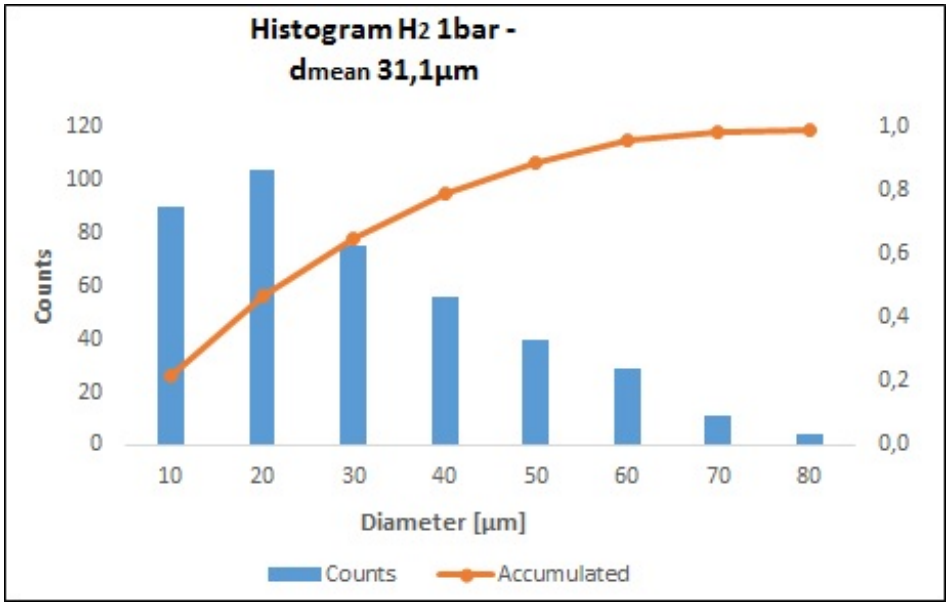

Figure 5.1: Histogram of H_2 bubble diameters at $1bar$

Figures (5.1) and (5.2) show the histogram of hydrogen bubbles at 1 and 100 *bar* respectively. The blue columns show the absolute frequency of bubbles occurring in certain range of diameter. The orange line cumulates the relative frequency to 100%.

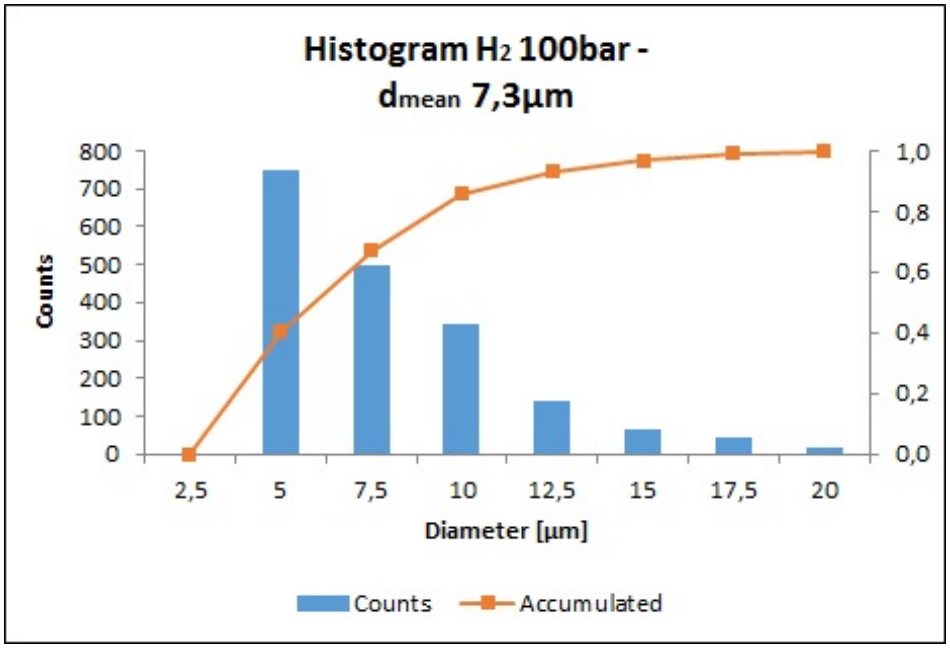

Figure 5.2: Histogram of H_2 bubble diameters at 100bar

Comparing the figures 5.1 and 5.2 it can be seen very clearly that not only the mean diameter changes significantly from 31.1μm at 1 bar to 7.3μm at 100 bar, but as well relative spread of diameters decreases. While at 1bar more than 90% of the bubbles are in the range between 0 and 70 μm, at 100 bar 90% of the bubbles are in the range between 0 and 17.5μm. However, the relative standard deviations remains quite constant at varying pressure such as the third statistical momentum, the skewness, which is always positive and takes values about 1.

With the optical measurement techniques (as described in 3.2.1) hydrogen bubbles can be detected up to a pressure of about 100 bar. At higher pressures the cloud of rising bubbles can not been analysed any more, because the bubble size gets to small and the limits of each particle can no be detected. The microscope and camera unit reaches its limits in visualization. Not only the camera limits but as well the borders of physics are reached as the laser wave has a length of 532nm.
Figure 5.3 shows the development of the mean bubble size of hydrogen, according to the operating pressure of the electrolyser. The data 1 to 100 bar is measured, the development up to 200bar is an extrapolation of the trend-line (see green line in Fig. 5.3)
Setting a trend-line for the evaluation of the mean diameter according to the pressure it

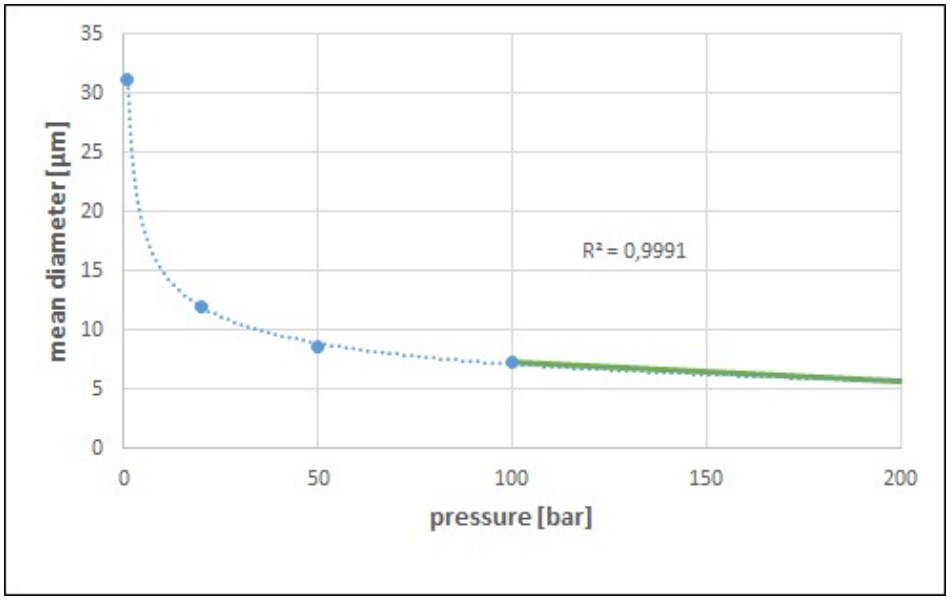

Figure 5.3: Pressure dependence of hydrogen bubble diameter

can be described in a good approximation with a potential development, described by the following equation:

$$\frac{d_{h_2,mean}}{\mu m}/ = 31.073 \cdot \frac{p}{bar}^{-0.319} \tag{5.1}$$

Oxygen

A histogram of each measurement series is made pointing out the frequency of distribution of the diameters occurring at a constant pressure. Furthermore the mean diameter is shown.

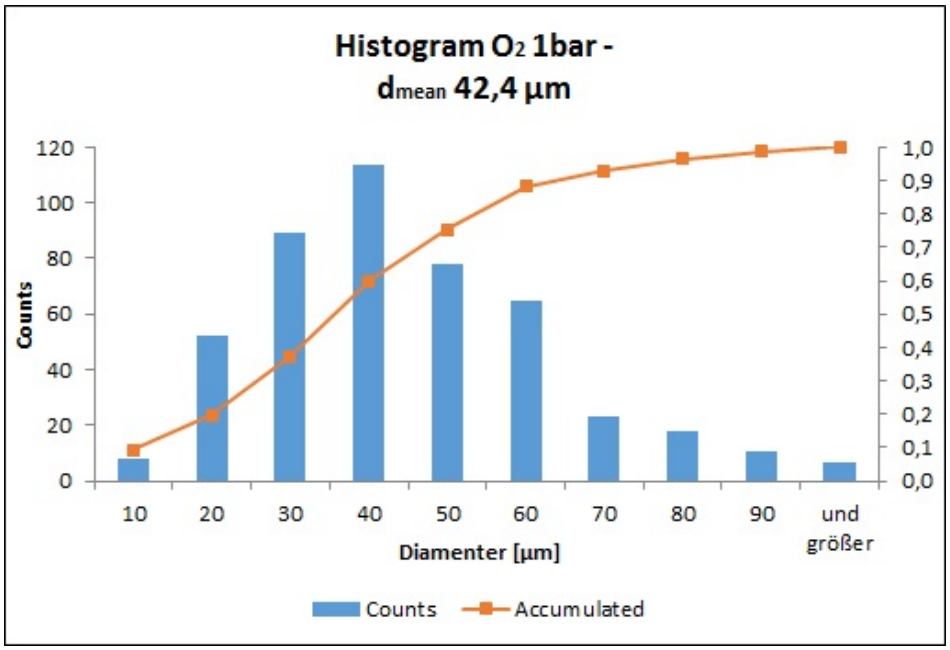

Figure 5.4: Histogram of O_2 bubble diameters at $1bar$

Figures 5.4 and 5.5 show the histogram of oxygen bubbles at 1 and 150 *bar* respectively. Similar to the histograms of the the hydrogen bubbles described before, the blue columns show the absolute frequency of bubbles occurring in certain range of diameter. The orange line cumulates the relative frequency to 100%.

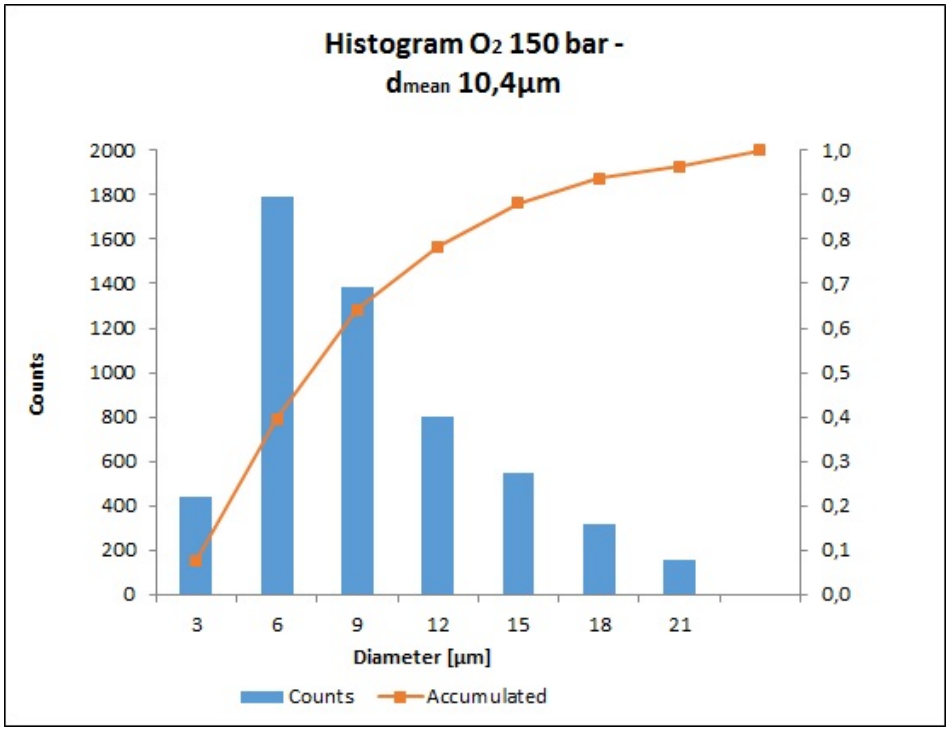

Figure 5.5: Histogram of O_2 bubble diameters at 150bar

Comparing the figures 5.4 and 5.5 very similar evaluation of the gas bubbles according to the pressure can be observed compared to the evaluation of hydrogen bubbles. Although oxygen bubbles provide a greater diameter than hydrogen ones at similar pressures but the tendency is the same. The mean diameter changes significantly from 24.4μm at 1 bar to 10.4μm at 150bar, but as well the range of diameters occurring decreases. While at 1bar more than 90% of the bubbles are in the range between 0 and 90 μm, at 100 bar 90% of the bubbles are in the range between 0 and 21μm. Similar to the statistics of hydrogen bubbles, the relative standard deviations remains quite constant at varying pressure such as the third statistical momentum, the skewness, which is always positive and takes values about 1.

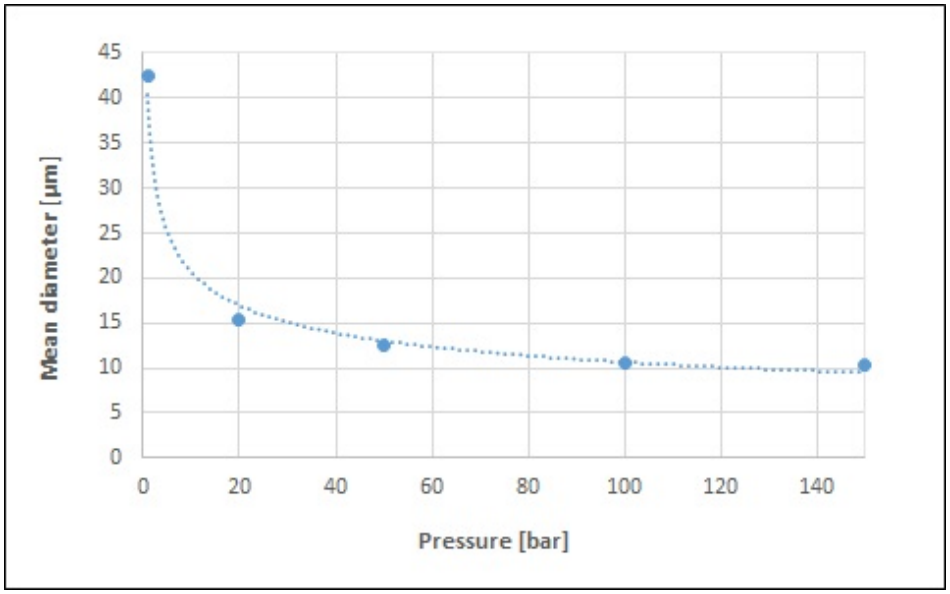

Figure 5.6: Pressure dependence of oxygen bubble diameter

Figure 5.6 and table 6.4 show the development of the mean bubble size of oxygen, according to the operating pressure of the electrolyser.
Setting a trend-line for the evaluation of the mean diameter according to the pressure it can be described in a good approximation with a potential development, described by the following equation:

$$\frac{d_{o2,mean}}{\mu m} = 40.34 \cdot \frac{p}{bar}^{-0.28} \tag{5.2}$$

5.2 Buoyant Velocity

Hydrogen

The result of the evaluation of the rising velocity c as function of the working pressure p is is listed in table 6.2 and graphically illustrated in the figure 5.7.

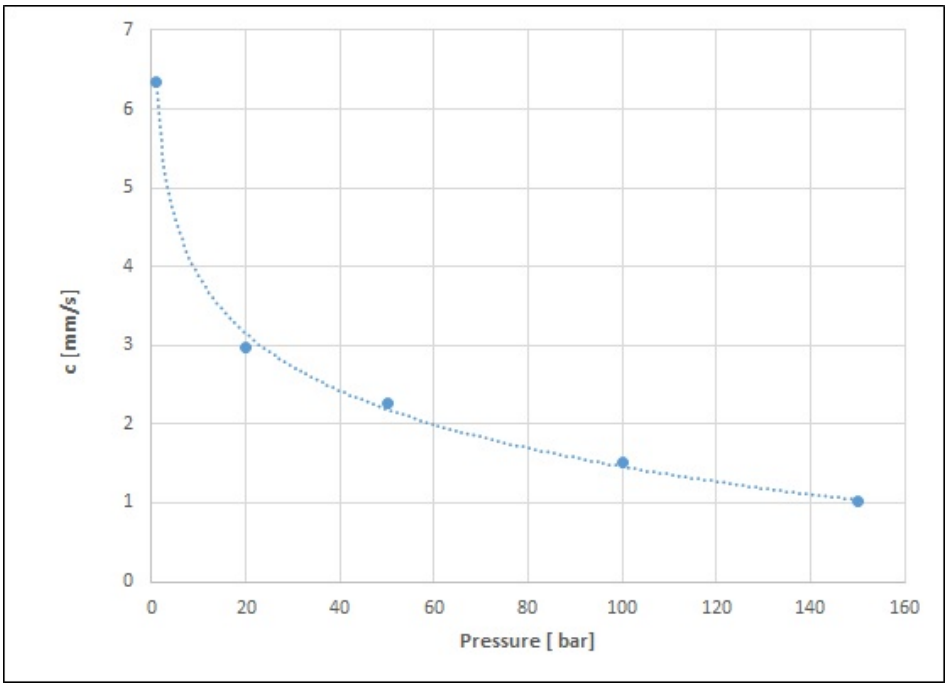

Figure 5.7: Development rising velocity/pressure hydrogen bubbles

The evaluation of the rising velocity in function of the pressure which is determined experimentally shows a logarithmic trend. Therefore a logarithmic trend-line is created which describes the detected dependency:

$$\frac{c_{h_2,mean}}{mm/s} = -1.05 \cdot ln(\frac{p}{bar}) + 6.29 \tag{5.3}$$

Oxygen

Similar as for the hydrogen bubbles, the result of the evaluation of the rising velocity c of the oxygen bubbles, in function of the working pressure p are graphically illustrated in the figure 5.8. The measured values are given in the appendix.

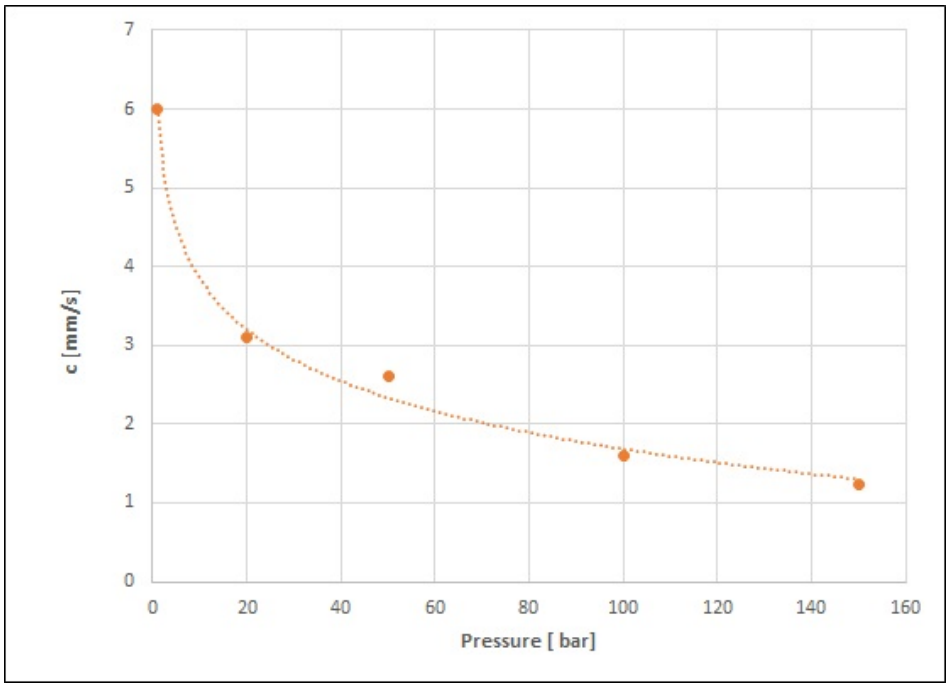

Figure 5.8: Development rising velocity/pressure oxygen bubbles

The evaluation of the rising velocity in function of the pressure which is determined experimentally shows a logarithmic trend. Therefore a logarithmic trend-line is derived which describes the detected dependency:

$$\frac{c_{o2,mean}}{mm/s} = -0.94 \cdot ln(\frac{p}{bar}) + 6.01 \tag{5.4}$$

5.3 Buoyant Velocity in Function of Bubble Size

As the bubble size as well as the buoyant velocity can be represented by a function depending on the working pressure of the electrolyser, it is possible to combine the two functions and describe the rising velocity in dependency of the gas bubble diameter. Following logarithmic expression are derived for hydrogen and oxygen.

$$\frac{c_{h_2,mean}}{mm/s} = 3.28 \cdot ln(\frac{d}{\mu m}) - 4.98 \tag{5.5}$$

$$\frac{c_{o_2,mean}}{mm/s} = 3.25 \cdot ln(\frac{d}{\mu m}) - 6.02 \tag{5.6}$$

The following figure shows the two equations. As negative rising velocities are non-physical the points where the buoyant velocity equals zero could be interpreted as critical diameter for the detachment diameter of respective gas.
Oxygen and hydrogen bubbles show a very similar behaviour. As the hydrogen gas has a lower density than oxygen, it possesses a higher rising velocity at similar diameters.

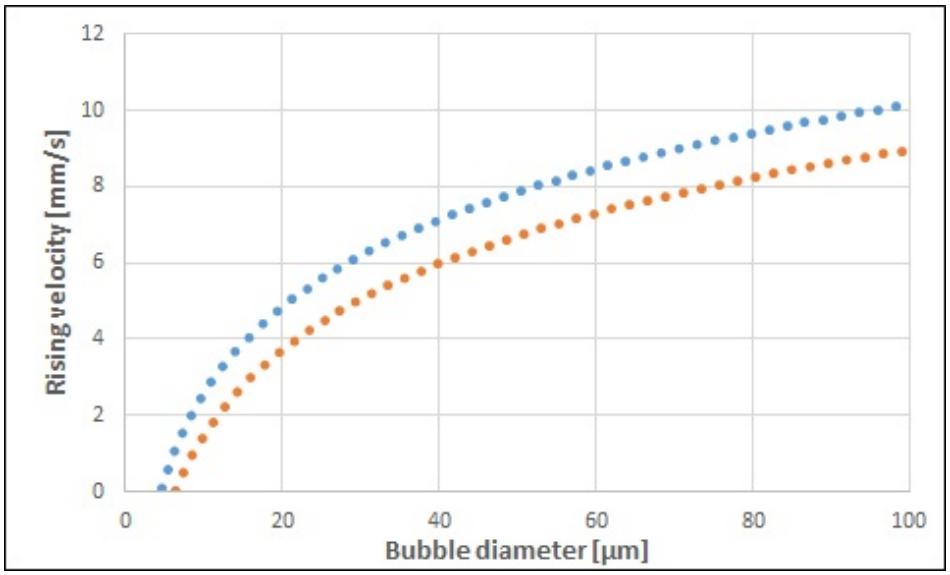

Figure 5.9: Rising velocyty of hydrogen and oxygen bubbles in function of their diameter

The derived correlation should be compared with stokes law. This way the viscosity of the electrolyte at the corresponding pressures could be evaluated.

6 Summary and Outlook

Due to the growing share of renewable energies, investigations on efficient energy storage are necessary in order store energy peaks as well as to transport large amount of energy. Hydrogen is an attractive option for energy storage with huge potential as it shows high energy efficiency, versatile use and good transportability.
Pressurising hydrogen to reach suitable storage pressure, requires a large percentage of stored energy. If the hydrogen production already provides high pressure, huge gains in system efficiency may be reached. This is the reason why high pressure electrolysers are an attractive solution.

The Institute of Nuclear and Energy Technologies (IKET) and the Instituto Tecnológigo de Buenos Aires (ITBA) work together in the design and construction of a high pressure alkaline electrolyser test cell. The particularity of the test cell is the working pressure up to 450 *bar* and windows in the taps for optical access.
The work of this master thesis describes the process of design and production of the device which has been realized in Buenos Aires and gives a indication about the safe operation of the equipment for further studies. Also the experiments performed at IKET and results are presented.

The experiments preformed and presented in this thesis, operate with a working pressure of the system between 1 and 150 *bar*. With a constant electrical direct current and constant electrolyte concentration the hydrogen and oxygen bubbles are analysed in respect to mean diameter and mean rising velocity.

Instructions for a standard operation procedure and a safe use of the electrolyter cell have been worked out and given in this work.

Experiments have shown, that the size of the bubbles present a potential development regarding rising working pressures, such as a significant decrease of the relative spread of the bubble diameters distribution with increasing pressures.
The rising velocity experiments show a logarithmic relation of buoyant velocity and working pressure.

As the bubble size such as the rising velocity depend on the working pressure, a relation between rising velocity and bubble diameter has been derived. A logarithmic function was found to describe this relation.
As this deduced function is a positive logarithmic equation, it has a negative value for bubbles which provide a very small diameter and are therefore not stable. This minimum diameter for hydrogen is about $5\mu m$, for oxygen it is about $6\mu m$. This may be interpretated as minimum detachment diameters.
The relation should be compared to Stokes' law.

The experiments executed and presented in this thesis are basic experiments in order to achieve first data and to test the operation of the device. As the operation of the electrolyser is very satisfactory, further and more detailed analysis can be made in a second stage of experimentation. One proposal is to repeat the described experiments with higher working pressure. Furthermore the impact of the ambient conditions like temperature, electricity density and concentration and purity of the electrolyte and the surface properties of the electrodes on the electrolysing process would be interesting to study.
In order to be able to analyse the bubbles' behaviour at higher pressures up to $450bar$ it is necessary to modify the optical installation and the analysing software, due to the fact that the optical equipment and software which has been used so far has come to its limits. As the produced bubbles tend to rise in clouds the difficulty occurring is to recognize the singles particles. The optical equipment is the most critical part for consecutive studies at higher pressures.

Bibliography

[1] Albers, Lauretta, Leslabay: *Electrolytic reactors for high pressure hydrogen generation, design and simulation*, ASME, 2008

[2] Lauretta: *Producción y almacenamiento de hydrógeno a alta presión*, Bar, 2007

[3] Onda et.al.: *Prediction of production power for high-pressure hydrogen by high-pressure water electrolysis*, Journal of Power Sources 132, 2004

[4] Zhang, Zeng: *Evaluating the Behavior of Electrolytic Gas Bubbles and Their Effect on the Cell Voltage in Alkaline Water Electrolysis*, American Chemical Society, 2012

[5] Sequeira et.al.: *Physics of Electrolyte Gas Evolution*, Sociedade Brasileira de Física, 2013

[6] C.A. Ward, A. Balakrishnan, F.C. Hooper, Trans. ASME 92, 695, 1970

[7] L.E. Scriven, Chem. Eng. Sci. 27, 1753, 1959

[08] D.E. Westerheide, J.W. Westwater, Am. Inst. Chem. Eng. J. 7, 357, 1961

[09] L.J.J. Janssen, S. van Stralen, Electrochim. Acta 26, 1011, 1981

[10] J. Venczel, Electrochim. Acta 15, 1909, 1970

[11] L.J.J. Janssen, J. Hoogland, Electrochim. Acta 18, 543, 1973

[12] C. Pfeifer, *Experimentelle Untersuchungen von Einflußfaktoren auf die Selbstzündung von gasförmigen und flüssigen Brennstofffreistrahlen*, KIT scientific reports 7555, 2010

[13] La Vision, *Product-Manual, ParticleMaster Shadow*, 2007

[14] T. Jordan, *Skript zur Vorlesung über Wasserstofftechnologie*, KIT 2013

Appendix

Tables

Table 6.1: Mean diameter of oxygen bubbles according to pressure

$p[bar]$	1	20	50	100	150
$d_{mean}[\mu m]$	42,4	15,3	12,6	10,6	10,4

Table 6.2: Mean diameter of hydrogen bubbles according to pressure

$p[bar]$	1	20	50	100
$d_{mean}[\mu m]$	31,1	12,0	8,6	7,3

Table 6.3: Mean velocity of hydrogen bubbles according to pressure

$p[bar]$	1	20	50	100	150
$c_{mean}[mm/s]$	6,3	3,0	2,3	1,5	1,0

Table 6.4: Mean velocity of oxygen bubbles according to pressure

$p[bar]$	1	20	50	100	150
$c_{mean}[mm/s]$	6,0	3,1	2,6	1,6	1,3

High Pressure Optical Electrolyser

STANDARD OPERATION PROCEDURE

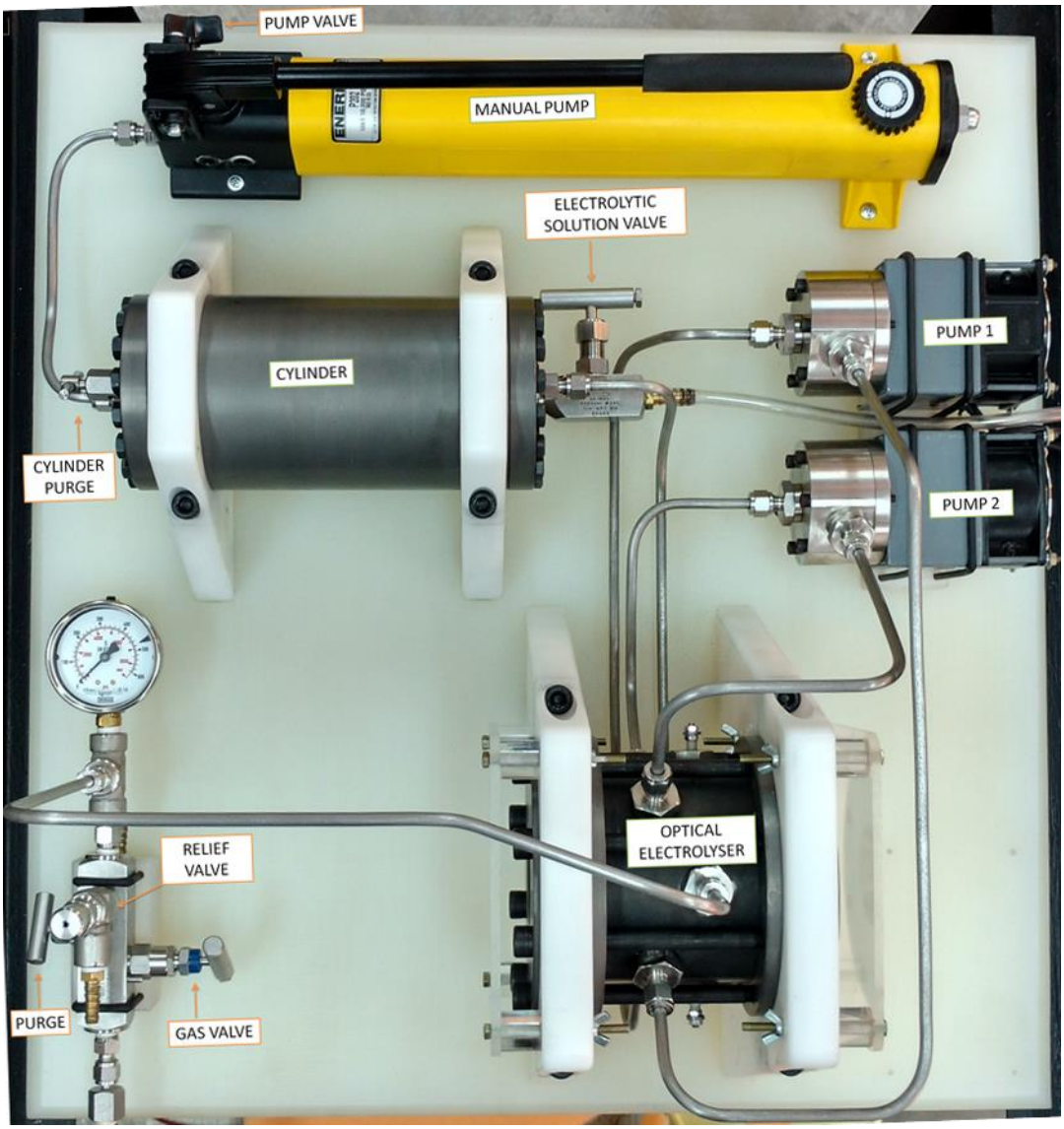

Device Description:

The 8 access ports in the pressure vessel allow for electric and hydraulic connections required. The different connectors have been provided to meet the established requirements.

Two system configurations have been established:

Medium pressure (200 bar): **The work pressure for this configuration cannot exceed 200 bar**. It includes two flanges with a wide optical access together with a set of M10x150 bolts and a relief valve set at 210 bar. Furthermore this system is fitted with two recirculation pumps which can be used to have a forced flow through the optical chamber.

High Pressure (450 Bar): **The work pressure for this configuration cannot exceed 450 bar.** It includes two flanges with a narrower optical access together with a set of M12x150 bolts and a relief valve set at 500 bar. This configuration must be used with pressures of up to 450 bar. **When this configuration is adopted, the recirculation pumps must not be connected.**

Going from one configuration to the other:

1. Make sure that the chamber is empty, has been completely depressurized (see D1/D2) and that the electrodes are unplugged.
2. Remove the safety acrylic glass and disconnect all the tube-connectors and the electrode wires.
3. Loosen the tank bolts (without taking them out)
4. Loosen the frame bolts.
5. Remove the upper frame of the supporting structure and place the tank on a safe and clean workbench with the bolts heads facing the roof, loosen them and take them out.
6. Carefully remove the flanges and place the new ones in the same manner,
7. Tightened the bolts progressively in small steps one bolt at a time until metal contact between the cylinder and the flanges has been achieved.
8. Torque all bolts to 15Nm
9. Place the tank on the frame and connect the tubing connectors or caps to the tank. **Make sure that the pumps are not linked to the tank if the configuration 2 is adopted.**
10. Once the tank and the tubing are in place, tighten the frame.
11. Finally, change the relief valve according to the configuration in place.

A. Required protection equipment.

- Ocular protection during experimentation and system set up is required at all times.
- Gloves and body overalls must be used when handling the electrolytic solution.

B. Required special supplies.

1- Electrolytic solution.
2- Nitrogen tank.
3- 900 cm^3 of hydraulic oil.
4- Facilities to charge hydraulic oil and electrolytic solution

C. System pressurization

1- Charge pump with 900 cm^3 of hydraulic oil. Make sure that when you put the lid back on the pump it is set in the venting position.
2- Retraction of piston: Verify that the purge valve, the electrolytic solution valve and the gas valve are closed and that the pump valve is open.
3- Connect the Nitrogen tank to the system.
4- Open the nitrogen tank bottle and set the gas pressure using the gas regulator.
5- Very gently, to avoid the hydraulic piston of hitting the back of the cylinder, open the gas valve, until the flow stops, ensuring a complete retraction of the piston.
6- Close the gas valve and depressurize the system by opening the purge valve;

7- With opened purge valve, open the electrolytic solution valve and pour the required amount of solution using a funnel; close the valve.
8- Close the purge valve.
9- Open the gas valve until the required initial pressure is reached.
10- Close the gas valve and the nitrogen tank valve.
11- Close the pump valve and make sure that the pump cap is in venting position.
12- Finally pump oil until the required pressure is reached.

D1. System depressurization (electrolytic solution volume unchanged)

1- Open partially the pump valve until the pressure of the hydraulic oil is relieved (avoid opening abruptly and make sure that the pump cap is in the venting position).
2- Close the pump valve.
3- Open the purge valve until the pressure of the chamber is completely relieved (according to the manometer lecture); close the purge valve.

D2. Despresurization with electrolytic solution emptying.

1- Open partially the pump valve until the pressure of the hydraulic oil is relieved (avoid opening abruptly and make sure that the pump cap is in venting the position).
2- Close the pump valve.
3- Open the purge valve until a pressure of 10 to 20 bar is reached.
4- Close the purge valve.
5- Make sure that you a wearing all the PPE required and proceed to carefully open the electrolytic solution valve to empty the required amount of electrolytic solution (do not open the valve abruptly to avoid splatter of the solution)
6- Close valve.

E. Change of electrodes

1- Before doing anything, make sure the entire system has been depressurized and that the electrolytic solution has been drained from the optical electrolyser.
2- Disconnect the electrodes from electric power source.
3- Unscrew electrodes and remove from the tank.
4- Clean electrodes of remaining electrolytic solution.
5- Unscrew and replace electrode tips.
6- Vary distance of electrode tips by removing/adding displacers.
7- Screw electrodes back in the tank.
8- Reconnect electrodes to the electric power source.
9- Pressurize the system and check leak tightness.

SAFETY DATA SHEET

SECTION 1: PRODUCT AND COMPANY IDENTIFICATION

Potassium Hydroxide

Product Name: Caustic Potash, Caustic Potash Flake, Caustic Potash Walnut, Caustic Potash 90%, Caustic Potash Briquettes 90%

Identified Uses: Chemical manufacturing, fertilizer, batteries, soaps

Company Information:
ASHTA Chemicals Inc.
P.O. Box 858
Ashtabula Ohio 44005
Phone: (440) 997-5221
Fax: (440) 998-0286
24-hour Emergency Phone: CHEMTREC: (800) 424-9300

SECTION 2: HAZARDS IDENTIFICATION

GHS Classification in accordance with 29 CFR 1910 (OSHA HCS)

GHS label elements, including precautionary statements:

Signal Word: **Danger**

Pictogram(s):

Hazard Statements	
H301	Toxic if swallowed.
H314	Causes severe skin burns and eye damage
H318	Causes serious eye damage.
H402	Harmful to aquatic life.
Precautionary Statements	
P260	Do not breathe dust/ fume/ gas/ mist/ vapors/ spray.
P264	Wash skin thoroughly after handling.
P273	Avoid release to the environment.
P270	Do not eat, drink or smoke when using this product.
P280	Wear protective gloves/eye protection/face protection.
P301 + P310	IF SWALLOWED: Immediately call a POISON CENTER or doctor/physician.
P301 + P330 + P331	IF SWALLOWED: Rinse mouth. Do NOT induce vomiting.

P303 + P361+ P353	IF ON SKIN (or hair): Remove/ Take off immediately all contaminated clothing. Rinse SKIN with water/ shower.
P305 + P351 + P338	IF IN EYES: Rinse cautiously with water for several minutes. Remove contact lenses, if present and easy to do. Continue rinsing.
P304 + P340	IF INHALED: Remove victim to fresh air and keep at rest in a position comfortable for breathing.
P310	Immediately call a POISON CENTER or doctor/ physician.
P321	Specific treatment (see supplemental first aid instructions on this label).
P390	Absorb spillage to prevent material damage.
P363	Wash contaminated clothing before reuse.
P405	Store locked up.
P406	Store in corrosive resistant stainless steel container with a resistant inner liner.
P501	Dispose of contents/container to an approved waste disposal plant.

SECTION 3: COMPOSITION/INFORMATION ON INGREDIENTS

Synonyms:

CHEMICAL NAME:	Potassium Hydroxide
TRADE NAME:	Caustic Potash, Caustic Potash Walnut, Anhydrous
SYNONYMS:	Caustic Potash, Potassium Hydrate, Lye, KOH
CONCENTRATION:	>90% potassium hydroxide (balance is moisture)
C.A.S:	1310-58-3
WHMIS:	D1B, E
CHEMICAL FORMULA:	KOH
CHEMICAL FAMILY:	Alkali

SECTION 4 FIRST AID MEASURES

Description of first aid measures:
Move out of dangerous area. Consult a physician. Show this safety data sheet to the doctor in attendance.

If inhaled
If breathed in, move person into fresh air. If breathing is difficult, give humidified air. Give oxygen but only by a certified physician. If breathing stops, provide artificial respiration. Get medical attention immediately.

In case of skin contact
Immediately take off all contaminated clothing. Wash off IMMEDIATELY with plenty of water for at least 15-20 minutes. Get medical attention. Wash clothing separately before reuse.
Destroy or thoroughly clean contaminated shoes.

In case of eye contact
Immediately flush eyes with plenty of water for at least 15 minutes. Remove contact lenses, if present and easy to do. Continue rinsing. Call a physician or poison control center immediately.

If ingested
Never give anything by mouth to an unconscious person. Rinse mouth with water. Give plenty of water to drink. Consult a physician.

SECTION 5 FIRE FIGHTING MEASURES

Flash Point:	Material is not flammable.
Extinguishing Media:	Use water spray, alcohol-resistant foam, dry chemical or carbon dioxide.
Auto Ignition Temp:	Non-combustible.
Special Fire Fighting Procedures:	Wear self-contained breathing apparatus and full protective clothing. In case of fire and/or explosion do not breathe fumes. Move containers from fire area if you can do so without risk. Use water spray to cool unopened containers.
Unusual Fire/Explosion Hazards:	Reacts with metals (aluminum, brass, copper, zinc, etc.) to generate flammable hydrogen gas, which then may cause fire and explosion.

SECTION 6 ACCIDENTAL RELEASE MEASURES

Environmental Precautions:
Do not discharge into drains, water courses or onto the ground.

Containment and Cleaning:
Cleanup personnel must wear proper protective equipment. Completely contain spilled material with dikes, sandbags, etc., and prevent any run-off into ground or surface waters or sewers. Recover as much material as possible into containers for disposal. Remaining material may be neutralized with dilute hydrochloric or acetic acid. Neutralization products, both liquid and solid, must be recovered for disposal.

Waste Control Procedures:
All disposals of this material must be done in accordance with federal, state and local regulations. Waste characterization and compliance with disposal regulations are the responsibilities of the waste generator.

SECTION 7: HANDLING AND STORAGE

Precautions to be taken for handling and storage:
This material generates considerable amounts of heat when added to water. Storage areas should be free of potential contact with acids, organics and reactive metals. Keep container tightly closed. Store in a cool, dry, well-ventilated place. Store in corrosive resistant container with a resistant inner liner. Store away from incompatible materials. Store at temperatures not exceeding 40°C/104°F. Compatible storage materials may include, but not be limited to, the following: nickel and nickel alloys, steel, plastics, plastic or rubber-lined steel, FRP or Derakane vinyl ester resin.

Precautions for repair:
Equipment: Only personnel trained and qualified in handling this product should prepare equipment for maintenance. Wash thoroughly with water.

Other Precautions: Spillage, when wet can be slippery. Potassium hydroxide is very hygroscopic and will become wet upon sitting in open moist air.

SECTION 8: EXPOSURE CONTROL/PERSONAL PROTECTION

Principal Component: Potassium Hydroxide

Occupational Exposure Limits:

ACGIH TLV	=	2 mg/m^3 (ceiling)
OSHA PEL	=	None
15 Minute STEL	=	None
NIOSH IDLH	=	None

Exposure Controls:

Eye Protection:	Chemical splash goggles and face shield.
Respiratory Protection:	None is normally required, however, if dusting, misting or heavy vapor formation should occur, a NIOSH approved respirator shall be worn.
Other Protection:	Rubber boots. Rubbers over leather shoes are not recommended. Rubber apron, rainwear or disposal tyvek suit with hard hat should be worn.
Ventilation Recommended:	Provide adequate ventilation to meet TLV requirements.
Glove Type Recommended:	Rubber, nitrile, neoprene, PVL.
Additional Information:	Safety eyewash/shower stations must be available in the work area.

Appropriate Engineering Controls:

Good general ventilation should be used. Ventilation rates should be matched to conditions. If applicable, use process enclosures, local exhaust ventilation, or other engineering controls to maintain airborne levels below recommended exposure limits. If exposure limits have not been established, maintain airborne levels to an acceptable level. Eye wash facilities and emergency shower must be available when handling this product.

SECTION 9: PHYSICAL AND CHEMICAL PROPERTIES

Information on basic physical and chemical properties:

Appearance	Whitish flake, walnut, pieces, etc.
Odor	No odor
Odor Threshold	Not available
pH	>14 (in aqueous solution)
Initial boiling point	1,320°C
Flash point	Not flammable
Evaporation rate	No data available
Flammability (solid, gas)	Not flammable
Upper/lower flammability or explosive limits	Not flammable
Autoignition Temperature	No data available
Water solubility	Very soluble
Physical State	Solid at room temperature
Molecular Weight	56.1
Melting Point	361°C
Specific Gravity (water = 1)	2.044 at 15.6°C (60°F)

Bulk Density	1,300 kg/m^3
Vapor Pressure	No data available
Vapor Density	No data available
Partition Coefficient: n-octanol/water	No data available

SECTION 10: STABILITY AND REACTIVITY

Stability:	Stable under normal condition.
Conditions to avoid:	Exposure to air can form potassium carbonate.
Incompatibility:	Organic chemicals, nitrocarbons, halocarbons and certain metals or alloys (aluminum, brass, copper, zinc, etc.). Oxidizing agents, acids. Initiates or catalyzes violent reactions of acetaldehyde, acrolein or acrylonitrile.
Hazardous decomposition products:	When KOH and certain metals (aluminum, brass, copper, zinc, etc.) react, hydrogen is generated which can be flammable or explosive.
Polymerization:	Hazardous polymerization will generally not occur.
Additional Information:	Trichlorethylene will react to form dichloracetylene, which is spontaneously flammable.

SECTION 11: TOXICOGICAL INFORMATION

Information on likely routes of exposure:

Skin Contact: Major potential hazard - contact with the skin can cause severe burns with deep ulcerations. Contact with solution or mist can cause multiple burns with temporary loss of hair at contact site. Solutions may not cause immediate pain or irritation upon skin contact. Prolonged or repeated contact with dilute solutions may cause drying and cracking of skin and possible skin damage.

Skin Absorption: It can penetrate to deeper layers of skin and corrosion will continue until removed. The severity of injury depends on the concentration and the duration of exposure.

Eye Contact: Major potential hazard – Liquid in the eye can cause severe destruction and blindness. These effects can occur rapidly affecting all parts of the eye. Mist or dust can cause irritation with high concentrations causing destructive burns.

Inhalation: By analogy with sodium hydroxide, inhalation of solution mist is expected to cause mild irritation at 2 mg/m^3. More severe burns and tissue damage in the upper respiratory tract can occur at higher concentrations. Pneumonitis can result from severe exposures.

Ingestion: Ingestion of potassium hydroxide can cause severe burning and pain in lips, mouth, tongue, throat and stomach. Severe scarring of the throat can occur after swallowing. Death can result from ingestion.

Information on toxicological effects:

Irritancy:	A study with a 10% solution showed severe tissue damage when applied to skin for 4 hours.
Sensitization:	Not available
Carcinogenicity:	Potassium hydroxide is not listed on the IARC, OSHA or NTP carcinogen lists.
Teratogenicity & Mutagenicity:	Not available
Reproductive Toxicology :	Not available
Toxicological Synergism :	Not available

Product Species Test Results:

LD_{50}: 333 mg/kg (rat oral)

LC_{50}: Fresh water mosquito fish: 80.0 mg/L (24 Hours, static)

SECTION 12: ECOLOGICAL INFORMATION

Ecological Information:

Persistence and degradability:	No data is available on the degradability of this product.
Bioaccumulative potential:	No data available for this product.
Mobility in soil:	Not available.
Other adverse effects:	No other adverse environmental effects (e.g. ozone depletion, photochemical ozone creation potential, endocrine disruption, global warming potential) are expected from this component.
Aquatic Toxicity:	May cause shifts in water pH outside the range of pH 7-9. This change may be toxic to aquatic organisms.

Biodegradability:

Not biodegradable (biodegradability term pertains to an organic material capable of decomposition as a result of attack by microorganisms). However, potassium hydroxide will be neutralized by acidity present in natural environment.

SECTION 13: DISPOSAL CONSIDERATIONS

Collect and reclaim or dispose in sealed containers at licensed waste disposal site if possible. Do not allow this material to drain into sewers/water supplies. Do not contaminate ponds, waterways or ditches with chemical or used container. Dispose of contents/container in accordance with local/regional/national/international regulations. Empty containers or liners may retain some product residues.

SECTION 14: TRANSPORT INFORMATION

Shipping:

Usual Shipping Containers:	Tank car, Tank truck, ABS Drums.
Usual Shelf Life:	Sealed containers, unlimited.
Storage/Transport Temperatures:	Ambient.

Suitable Storage:

Materials/Coatings:	Steel, plastic, polyethylene (when dry).

Unsuitable: Aluminum or galvanized containers.

D.O.T. Information:
UN number: 1813
Class: 8
Packing group: II
Proper shipping name: Potassium Hydroxide, solid
Reportable Quantity (RQ): 1000 lbs (100% KOH basis)
Marine pollutant: No Poison Inhalation Hazard: No

SECTION 15 REGULATORY INFORMATION

SARA 302 Components
SARA 302: Not listed.

SARA 313 Components
SARA 313: Not regulated.

SARA 311/312 Hazards
Acute health hazard.

Massachusetts Right To Know Components
Potassium Hydroxide CAS#: 1310-58-3

Pennsylvania Right To Know Components
Water CAS#: 7732-18-5
Potassium Hydroxide CAS#: 1310-58-3

New Jersey Right To Know Components
Water CAS#: 7732-18-5
Potassium Hydroxide CAS#: 1310-58-3

California Prop. 65 Components
This product does not contain any chemicals known to state of California to cause cancer, birth defects, or any other reproductive harm.

OSHA PSM TPQ: Not listed

Toxic Substances Control Act (TSCA):
CAS# 1310-58-3 is listed on the TSCA inventory.

Comprehensive Environmental Response Compensation Liability Act: (CERCLA)
CAS# 1310-58-3 is listed on the CERCLA list.

SECTION 16 OTHER INFORMATION

NFPA Rating:
Health Hazard: 3
Fire Hazard: 0
Reactivity Hazard: 1

HMIS Rating:
Health Hazard: 3
Chronic Health Hazard:
Flammability: 0
Physical Hazard: 1

This information is drawn from recognized sources believed to be reliable. ASHTA Chemicals, Inc. Makes no guarantees or assumes any liability in connection with this information. The user should be aware of changing technology, research, regulations, and analytical procedures that may require changes herein. The above data is supplied upon the condition that persons will evaluate this information and then determine its suitability for their use. Only U.S.A regulations apply to the above.

Version 1.0	For the new GHS SDS Standard	Revision Date: 2/4/2015
Version 1.1	Graphics updated	Revision Date: 3/9/2015
Version 1.2	Description update	Revision Date: 4/20/2015
Version 1.3	Changes to Sections 1, 9	Revision Date: 7/29/2015